Continuous facility location with backbone network costs

John Gunnar Carlsson and Fan Jia*

June 6, 2013

Abstract

We consider a continuous facility location problem in which our objective is to minimize the weighted sum of three costs: fixed costs from installing the facilities, backbone network costs incurred from connecting the facilities to each other, and transportation costs incurred from providing services from the facilities to the service region. We first analyze the limiting behavior of this model and derive the two asymptotically optimal configurations of facilities: one of these configurations is the well-studied *honeycomb heuristic*, while the other is an Archimedean spiral. We then give a fast constant-factor approximation algorithm for finding the placement of a set of facilities in any convex polygon that minimizes the sum of the three aforementioned costs.

1 Introduction

Broadly speaking, a set of facilities providing service to a geographic region often incurs costs from three major sources:

1. *Fixed costs* from installing the facilities,
2. *Backbone network* costs from connecting the facilities to each other, and
3. *Transportation costs* from providing services from the facilities to the region.

Letting $X = \{x_1, \ldots, x_k\}$ denote the set of facilities and R the service region, the optimal location problem is therefore given by

$$\underset{X}{\text{minimize}}\ \text{Fixed}(X, R) + \text{Backbone}(X, R) + \text{Transportation}(X, R)\,. \tag{$*$}$$

The novelty of problem $(*)$ comes from the property that the fixed and backbone network costs will often increase as more facilities X are added (since increasing the number of facilities in a region usually increases the fixed costs in the region and makes the backbone network longer, although exceptions to this principle certainly exist), but the transportation costs should decrease because there are more facilities located in the region to provide service. In this paper, we consider the case where the service region is a convex polygon C and the facilities X represent facilities whose customers or clients are uniformly distributed in the region. An application of $(*)$ was introduced in [6] where the goal is to minimize the total amount of carbon emissions that are produced by a supply chain network of retail stores and the customers they serve. In this paper we approximate the three quantities above by making the following assumptions:

1. The costs due to *facilities* (the "fixed costs") take the form $\gamma_k \cdot k$, where $k = |X|$ and $\{\gamma_k\}$ is a sequence whose k-th entry γ_k represents the fixed cost per facility when we build a total of k facilities. It is natural to assume that γ_k is decreasing to reflect the intuitive notion that a collection of small facilities is cheaper per facility (or "produces fewer emissions per facility", in the language of [6]) than a single, large, central facility (e.g. a single facility with capacity to serve 1000 customers produces more emissions than a facility with capacity to serve only 500 customers). It is also natural to suppose that $\gamma_k \cdot k$ should *increase* as k becomes larger, due to the usual economies of scale (e.g. a single facility with capacity to serve 1000 customers produces fewer emissions than *two* facilities each having capacity to serve 500 customers).

*Department of Industrial and Systems Engineering, University of Minnesota. The authors gratefully acknowledge DARPA Young Faculty Award N66001-12-1-4218, NSF grant CMMI-1234585, and ONR grant N000141210719.

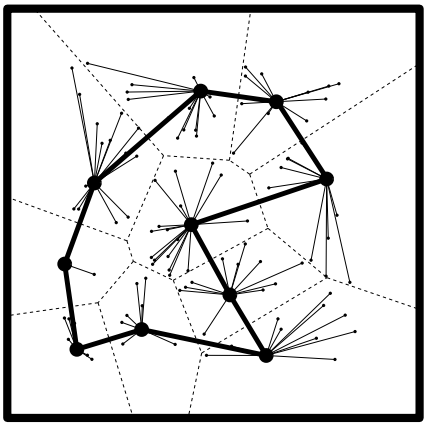

Figure 1: The relevant quantities in objective function (1) where C is a square. The thick black lines indicate the backbone network (a TSP tour), the large points indicate facilities X, the small points indicate various customer locations (which we do not deal with explicitly in our formulation, as they are assumed to be continuously and uniformly distributed in the region), and the dashed lines indicate the service sub-regions (i.e. the Voronoi cells) of the facilities.

2. The costs due to the *backbone network* are proportional to $\mathrm{TSP}(X)$, a travelling salesman tour of X. This models the case where a single warehouse (coincident with one of the facilities) supplies goods to the facilities X using a single truck to transport goods from the warehouse to the facilities. This transportation is facilitated via linehaul transportation on a so-called *peddling* route [19], that is, a route consisting of multiple stops.

3. The costs due to *transportation* from the facilities to the service region are proportional to $\mathrm{Dir}(X, C) := \iint_C \min_i \|x - x_i\| \, dA$, that is, the average length of a direct trip between a point x sampled uniformly in C and its nearest facility x_i (scaled proportionally to the area of C). This models the case where we have a continuum of customers distributed uniformly in C and each one uses their nearest facility, making a single direct round trip to and from the facility. In order to emphasize that the trip consists of both an outbound and an inbound leg, it is perhaps more appropriate to model the local transportation costs as $2 \cdot \mathrm{Dir}(X, C)$; in order to keep our notation compact, we will suppress the coefficient "2" and assume that it is included in the relevant input parameters, which are introduced in the next paragraph.

It follows that we can model the total costs due to the facilities X providing service to customers in C as

$$F(X) = \gamma_{|X|} \cdot |X| + \phi \, \mathrm{TSP}(X) + \psi \, \mathrm{Dir}(X, C) \tag{1}$$

where $\{\gamma_k\}$ is a given sequence and ϕ and ψ are given constants; see Figure 1. The salient property of this model is that linehaul transportation via the backbone network benefits from an *economy of scale* because a TSP tour of the points X has decreasing marginal costs as $|X|$ becomes larger (see [2], for example, which explains that for uniformly distributed point sets X, the length of $\mathrm{TSP}(X)$ increases proportionally to $\sqrt{|X|}$ as $|X| \to \infty$). On the other hand, the local transportation costs are modelled via direct trips and thus the workload at each facility does not benefit from such an economy of scale. This model might be contrasted with [12], which uses peddling routes (i.e. diminishing marginal returns) in both the backbone network and in the local transportation, or [7], which uses direct routes in the backbone network but peddling routes in the local transportation (the exact opposite of our setting). One natural instance of our problem arises when one considers the problem faced by stores selling items that require delivery or installation, such as appliances, electronics, food, or furniture: large freight trucks distribute products to showrooms, which are then put on display to customers. These customers then schedule a delivery and installation of their desired product. Because of the time-sensitivity of such requests and other complications, economies of scale are much harder to leverage at the local store-to-customer level than at the transshipment level (the paper [7], for example, quantifies this when one of the "complications" considered is capacities on the second-stage vehicles). In our work we make this distinction clear by modelling the facility-to-customer transportation costs using direct trips from facilities to customers, but modelling the backbone network linehaul between facilities using peddling routes. In Section 2.1 we show how to generalize this model

Parameter	Units	Comments
γ_k	$\frac{\text{cost/facility}}{\text{week}}$	when k facilities are providing service
ϕ	$\frac{\text{cost}}{\text{mile}} \cdot \frac{\text{\# trips required}}{\text{week}}$	for trucks on the backbone network
ψ	$2 \cdot \frac{\text{cost}}{\text{mile}} \cdot \frac{\text{(\# trips required)/customer}}{\text{week}} \cdot (\text{\# customers})$	for customers in C

Table 1: Units of the parameters γ_k, ϕ, and ψ in the formulation (1). Note that the term "# trips required" may differ from ϕ to ψ, which models the case where the frequency of trips between the facilities and the customers is different from the frequency of trips along the backbone network. Note also the coefficient "2" of ψ, which reflects the assumption that transportation between facilities and customers occurs via direct trips to and from the facility. The model introduced in [6] measures "cost" in terms of pounds of CO_2.

to address the case where facility-to-customer transportation costs are incurred using multi-stop trips instead of direct trips under certain assumptions on the lengths of these multi-stop trips.

The units of the problem input parameters are given in Table 1, which takes into account the fact that the frequency of trips between the facilities and customers may differ from trips along the backbone network. We re-iterate that we allow $k = |X|$ to vary also, i.e. to choose how many facilities to build. This objective function[1] was first introduced in [6], in which the author uses several regular polygonal tilings of the plane to estimate the "carbon penalty" of facility configurations, that is, the difference between the carbon cost to a firm and the true externality cost of the total emissions generated. The author shows that, using reasonable estimates of the input parameters, the realized penalty is negligible. In this paper we make two contributions: in Section 2 we analyze the objective function (1), and we show that an asymptotically optimal configuration is to distribute the facilities either in a hexagonal tiling or equidistantly along an Archimedean spiral, depending on the nature of the input parameters. Next, we derive two lower bounds for the function (1) for a given convex region C, which we use in a constant-factor approximation algorithm for placing the points X in C so as to minimize the total cost of the facility configuration.

Other applications

It is worth mentioning that the objective function (1) is a sensible model for carbon emissions as in [6], but also works more generally as a model for spatial one-to-many distribution models with transshipment; elements of such models have previously been examined in [7, 8, 15], for example. Rather than minimizing emissions, one might attempt to minimize the actual financial costs incurred by the company in placing its retail stores, warehouses, or other such facilities. In this case, the fixed and backbone network costs are easily understood, though the transportation costs in (1) do not have an obvious counterpart because customers generally bear the cost of travel to retail stores rather than vice versa (with exceptions being businesses that primarily deliver goods to their customers such as large appliances, electronics, food, or furniture), so the company does not directly incur the cost $\psi \operatorname{Dir}(X, C)$. In such a case, we should use an alternative model for the transportation costs that possesses some kind of spatial demand component (i.e. that customers near a facility are more likely to use it than those farther away); we will discuss one such model in Section 2.1.

One might also consider applying this model to the design of an urban transportation network, such as a high-speed rail line. The major difference in this case is that high-speed rail is, for the most part, a "many-to-many" phenomenon, which is distinct from our problem. Our model would perhaps be best suited for the case where a large collection of passengers emanates from a single source, such as a central business district. In this case, rather than using a travelling salesman tour as a backbone network, we might use a minimum spanning tree or a Steiner tree. Our analysis here actually carries over to these alternative backbone networks as well, and we discuss them where appropriate.

Related work

The canonical location problem that is most closely related to (∗) is clearly the *uncapacitated facility location problem* [20], although the two differ substantially by the inclusion of backbone network costs. A more directly related model to (∗) is in the seminal paper [21], which describes several discrete and continuous models and algorithms for simultaneous facility location and routing. The first explicit formulation of (∗) to our knowledge is found in [22], which demonstrates

how to solve a hybrid location/routing location problem on a graph as a mixed integer program; further developments on network formulations of problems of type $(*)$ have since emerged [1, 23].

The formulation (1) has previously been discussed (but not solved) in [19], which gives a taxonomy of six classes that differentiate the various continuous approximation models developed for freight distribution problems. The problem of minimizing objective function (1) belongs to class IV, "one-to-many distribution with transshipments", which we can readily observe in Figure 2 of that paper. One important distinction between the models of [19] and our own is that we use the expression $\mathrm{Dir}(X, C) = \iint_C \min_i \|x - x_i\| \, dA$ to model the transportation costs, whereas the corresponding models in [19] use travelling salesman tours originating at the facilities. In Section 2.1 we will show that the conclusions we derive here are more or less applicable to the approach used therein. Along the same lines, Sections 5 and 6 of [25] provide an elegant theoretical justification, using continuum mechanics, for the continuous approximation that this paper employs to describe approximate global optima to the objective functions used herein.

A relatively new branch in location theory deals with *location-routing* problems (LRP) that pay special attention to vehicle routing issues in facility placement [24]. Such problems are substantially more difficult than the canonical location models because, as the paper [4] observes,

> [T]he facility...must be "central" relative to the ensemble of the demand points, as ordered by the (yet unknown) tour through all of them. By contrast, in the classical problems the facility...must be located by considering distances to individual demand points, thus making the problem more tractable.

One important distinction between the LRP and our problem $(*)$ is that we think of the backbone network as connecting the *facilities* together, whereas the LRP considers networks that connect the *customers* together (i.e. vehicle tours that provide service to the customers). In our formulation (1), a parallel argument to the quotation above would be as follows: minimizing the transportation costs, $\mathrm{Dir}(X, C)$, would dictate that we should spread the facilities X as uniformly as possible throughout C, and thus be "central" with respect to the customers. However, by pursuing such a strategy too aggressively, we incur large fixed and backbone network costs $\gamma_{|X|} \cdot |X| + \phi \, \mathrm{TSP}(X)$.

Section 2 of this paper studies the limiting behavior of the optimal solution to our problem (1) as the transportation coefficient ψ becomes large. As such, our analysis closely resembles other research on the asymptotic behavior of Euclidean optimization problems, such as the travelling salesman problem [2, 5, 17] and general *subadditive Euclidean functionals* [28, 31] as well as the *k-center* and *k-medians* problems [18, 32]. Although our analysis is deterministic (as opposed to the cited works which are probabilistic), the spirit of our contribution is most closely related to the aforementioned results.

Notational conventions

A quantity that we will use frequently in this paper is the *Fermat-Weber value* of a shape S, $\mathrm{Dir}(S)$, which refers to the quantity

$$\mathrm{Dir}(S) = \min_{x_0 \in S} \iint_S \|x - x_0\| \, dA \,,$$

so that x_0 is the point that minimizes the average direct-trip distance between a uniformly selected point in S, i.e. x_0 is the *geometric median* of S. For any shape S we define $\mathrm{diam}(S)$ to be the *diameter* of S, i.e. $\max_{x,y \in S} \|x - y\|$. For any shape S and any point x_0, we define the distance function

$$D(x_0, S) = \min_{x \in S} \|x - x_0\|$$

and for any set $S \subset \mathbb{R}^2$, let $N_\epsilon(S)$ denote the set of all points x within ϵ of S, i.e. $N_\epsilon(S) = \{x : D(x, S) \leq \epsilon\}$. For any (possibly infinite) set of points X in a convex region C, we define

$$\mathrm{Dir}(X, C) = \iint_C \min_{x' \in X} \|x - x'\| \, dA \,.$$

For any scalar x, we let $\lfloor x \rfloor$ and $\lceil x \rceil$ denote the floor and ceiling functions of x, we let $\lfloor x \rceil$ denote the rounding function of x, and we let $\log(x)$ denote the natural log of x. Finally, we shall make use of four common conventions in asymptotic analysis:

- We say that $f(x) \in \mathcal{O}(g(x))$ if there exists a constant c and a value x_0 such that $f(x) \leq c \cdot g(x)$ for all $x \geq x_0$,

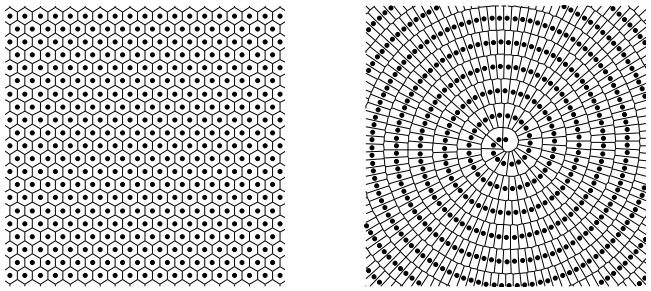

(a) (b)

Figure 2: Facility placement using the two asymptotically optimal configurations, the honeycomb heuristic and the Archimedes heuristic.

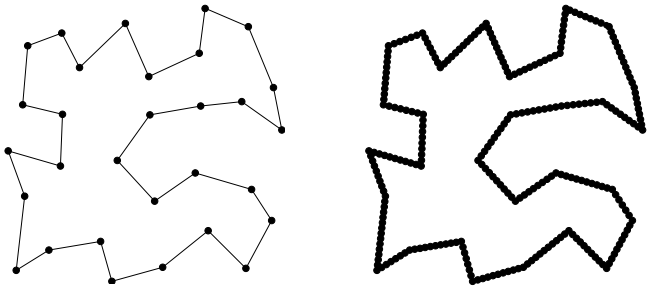

(a) (b)

Figure 3: If $\gamma_k = 0$ for all k, then the absence of fixed costs for facilities implies that configuration (3a) is strictly worse than (3b); that is, we should place infinitely many facilities along the backbone network.

- We say that $f(x) \in o(g(x))$ if $\lim_{x\to\infty} f(x)/g(x) = 0$,
- We say that $f(x) \in \omega(g(x))$ if $\lim_{x\to\infty} f(x)/g(x) = \infty$, and
- We say that $f(x) \sim g(x)$ if $\lim_{x\to\infty} f(x)/g(x) = 1$.

2 Asymptotic analysis

We shall begin by considering the optimal configurations for minimizing (1) as the various parameters γ_k, ϕ, and ψ change; without loss of generality we assume that $\text{Area}(C) = 1$. As $\psi \to 0$, representing a very sparsely populated region in which the transportation cost to consumers becomes negligible, the optimal configuration is clearly to place a single facility ($k = 1$) in the region C. We shall devote most of this section to the impact of increasing population density, i.e. $\psi \to \infty$, although before doing so we will consider two special cases of (1):

The case $\phi = 0$ If $\phi = 0$, then we do not incur any penalty for the backbone network $\text{TSP}(X)$ of X. The optimal number of points k to place will depend on the behavior of γ_k, but clearly once we have selected k our objective is merely to distribute those k points as uniformly as possible in C (minimizing $\text{Dir}(X, C)$), without regard to their backbone network. We thus have a kind of "soft constrained" instance of the well-studied *k-medians* problem, and as the optimal k becomes large (equivalently, as $\psi \to \infty$), the optimal solution is known to be the *honeycomb heuristic* [18, 25] which is shown in Figure 2a.

The case $\gamma_k = 0$ If $\gamma_k = 0$ for all k, then we do not incur any penalty for placing facilities in the region if they do not lengthen the backbone network. Thus, our optimal configuration will be to place infinitely many facilities along the

backbone network (see Figure 3), although we have not yet discussed what the shape of the backbone network should be. One possibility is to use an *Archimedean spiral*, shown in Figure 2b, with equation given in polar coordinates as $r = a\theta$. In Section A of the online supplement we show that by setting $a = \sqrt{\phi/\psi}/\pi$, the length of the backbone network is $\mathrm{TSP}(X) \sim \frac{\sqrt{\psi/\phi}}{2}$ and therefore that the overall cost, $\phi\,\mathrm{TSP}(X) + \psi\,\mathrm{Dir}(X, C)$, approaches $\sqrt{\phi\psi}$. Using a lower bound, we will show in Section 3 that this configuration, which we call the "Archimedes heuristic", is actually optimal as $\psi \to \infty$. The Archimedean spiral was previously identified as being an optimal configuration for a related sensor location problem described in [9]; in that paper, rather than explicitly incurring backbone network costs $\phi\,\mathrm{TSP}(X)$, the objective is to determine a policy for a collection of mobile robots with limited communication radii to convene into a configuration such that all robots can communicate with one another. It turns out that the spiral parameter a varies on the communication radii of the robots.

For notational simplicity, we assume for the remainder of this section that $\phi = 1$ (this is done without loss of generality since we are examining the limiting behavior as $\psi \to \infty$). Having discussed the two preceding cases we shall now sketch a proof of the following claims, which relate γ_k and ψ:

Claim 1. Suppose that $\gamma_k \in \omega(k^{-1/2})$. As $\psi \to \infty$, the honeycomb heuristic (with appropriately chosen values of $k = |X|$) is an asymptotically optimal configuration for minimizing (1).

Claim 2. Conversely to Claim 1, if $\gamma_k \in o(k^{-1/2})$, then as $\psi \to \infty$, the Archimedes heuristic (with appropriately chosen values of $k = |X|$) is an asymptotically optimal configuration for minimizing (1).

We will prove Claim 1 first by showing that, as $\psi \to \infty$, the backbone network cost $\mathrm{TSP}(X)$ is dwarfed by the fixed costs $\gamma_{|X|} \cdot |X|$ and the facility-to-customer transportation cost $\psi\,\mathrm{Dir}(X, C)$. Let $k(\psi)$ denote the optimal number of facilities that we should place if our objective is merely to minimize $\gamma_{|X|} \cdot |X| + \psi\,\mathrm{Dir}\,(X, C)$, i.e. assuming $\phi = 0$ (these must be in a honeycomb configuration, by our earlier argument). Consider the objective cost of a honeycomb configuration of $k(\psi)$ facilities, but with $\phi = 1$ as in our original assumption:

$$\gamma_{k(\psi)} \cdot k(\psi) + \mathrm{TSP}(X) + \psi\,\mathrm{Dir}(X, C)$$

(for clarification, we re-iterate that, in the above expression, $k(\psi)$ is always defined by assuming $\phi = 0$). Since the Fermat-Weber value of a hexagon H with unit area is given by

$$\alpha_1 := \mathrm{Dir}\,(H) = \frac{3^{3/4}\,(4 + 3\log 3)\,\sqrt{6}}{108} \approx 0.37721,$$

it is straightforward to see that the Fermat-Weber value of a regular hexagon with area A is $\alpha_1 A^{3/2}$. In our case we have $k(\psi)$ hexagons with area $1/k(\psi)$ and therefore the total Fermat-Weber value of our $k(\psi)$ facilities is simply $k(\psi) \cdot \alpha_1\,(1/k(\psi))^{3/2} = \alpha_1/\sqrt{k(\psi)}$. Each of these hexagons has sides of length $(\sqrt{2}/3^{3/4}) \cdot (1/\sqrt{k(\psi)})$ and therefore each point has an associated TSP tour segment of length $\beta_1/\sqrt{k(\psi)}$, with $\beta_1 := 3^{-1/4}\sqrt{2} \approx 1.0746$. We therefore find that, as $\psi \to \infty$, $k(\psi)$ becomes large, and therefore the objective function value $F(X)$ approaches

$$F(X) \sim \gamma_{k(\psi)} \cdot k(\psi) + \beta_1\sqrt{k(\psi)} + \psi\alpha_1/\sqrt{k(\psi)}\,.$$

Since $\gamma_k \in \omega(k^{-1/2})$, or equivalently $\gamma_k \cdot k \in \omega(\sqrt{k})$, we can select a value of ψ large enough so that $k(\psi)$ becomes sufficiently large as to force the quantity

$$\frac{\beta_1\sqrt{k(\psi)}}{\gamma_{k(\psi)} \cdot k(\psi)}$$

to be arbitrarily small. The ratio

$$\frac{\gamma_{k(\psi)} \cdot k(\psi) + \beta_1\sqrt{k(\psi)} + \psi\alpha_1/\sqrt{k(\psi)}}{\gamma_{k(\psi)} \cdot k(\psi) + \psi\alpha_1/\sqrt{k(\psi)}}$$

therefore converges to 1, which proves the asymptotic optimality of the honeycomb heuristic since the denominator of the above expression is clearly a lower bound for our original problem.

To prove Claim 2, we consider a set X of k points distributed equidistantly in C along an Archimedean spiral having length ℓ. As k becomes large, the Voronoi cells of these points can be approximated by rectangles R_i having dimensions

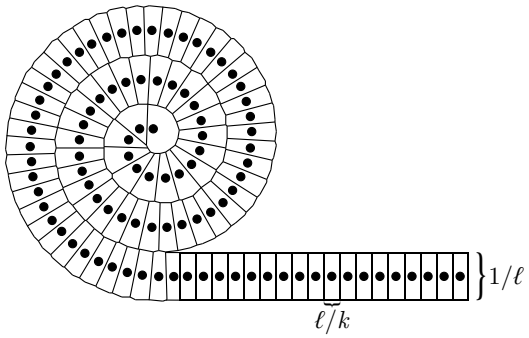

Figure 4: For a sufficiently long spiral it is easy to see that the Voronoi cells of each point are approximately rectangular, with dimensions $\ell/k \times 1/\ell$ (this is because there are k such cells and we assume that the area of C is 1).

$\ell/k \times 1/\ell$, as shown in Figure 4. We can approximate the Fermat-Weber value of such a rectangle as follows:

$$\mathrm{Dir}(R_i) = \int_{-1/(2\ell)}^{1/(2\ell)} \int_{-\ell/(2k)}^{\ell/(2k)} \sqrt{x^2+y^2}\, dx\, dy \approx \int_{-1/(2\ell)}^{1/(2\ell)} \int_{-\ell/(2k)}^{\ell/(2k)} |x| + |y|\, dx\, dy = \frac{1}{4k\ell} + \frac{\ell}{4k^2}$$

so that $\mathrm{Dir}(X,C) \approx k \cdot \mathrm{Dir}(R_i) \approx 1/4\ell + \ell/4k$ (our assumption that k is large means that the R_i's will be skinny, which justifies our approximation of the integrand $\sqrt{x^2+y^2} \approx |x| + |y|$ above). When we set $\ell = \sqrt{\psi}/2$ (which is equivalent to using $a = \sqrt{1/\psi}/\pi$ in the polar equation $r = a\theta$) we find that $\mathrm{Dir}(X,C) \sim 1/2\sqrt{\psi} + \sqrt{\psi}/8k$, so that the total objective cost is

$$F(X) \approx \gamma_k \cdot k + \underbrace{\sqrt{\psi}/2}_{\mathrm{TSP}(X)} + \psi \underbrace{\left(\frac{1}{2\sqrt{\psi}} + \frac{\sqrt{\psi}}{8k}\right)}_{\mathrm{Dir}(X,C)} = \gamma_k \cdot k + \sqrt{\psi} + \frac{\psi^{3/2}}{8k}\,.$$

Note that the above expression depends only on $\{\gamma_k\}$ and ψ, which are given, and k, which we are free to choose. Using the fact that $\gamma_k \in o(k^{-1/2})$, or equivalently $\gamma_k \cdot k \in o(\sqrt{k})$, we will show that

$$\lim_{\psi\to\infty} \min_k \gamma_k \cdot k + \sqrt{\psi} + \frac{\psi^{3/2}}{8k} \sim \sqrt{\psi}$$

or equivalently that

$$\lim_{\psi\to\infty} \min_k \gamma_k \cdot k + \frac{\psi^{3/2}}{8k} \in o(\sqrt{\psi})\,.$$

Suppose for a contradiction that the above limit does not hold. If this is the case, then there exists a constant $c > 0$ and an increasing sequence $\{\psi_i\} \to \infty$ such that

$$\gamma_k \cdot k + \frac{\psi_i^{3/2}}{8k} \geq c\sqrt{\psi_i} \tag{2}$$

for all i and k. As $\gamma_k \cdot k \in o(\sqrt{k})$, there exists a threshold $\bar{k}$ such that $\gamma_k \cdot k < (c^{3/2}/8)\sqrt{k}$ for all $k \geq \bar{k}$. Now set $k^* = 4\psi_i/c$ and assume without loss of generality that $k^* \geq \bar{k}$ (otherwise we simply remove the first few elements of the sequence $\{\psi_i\}$) We find that

$$\gamma_{k^*} \cdot k^* + \frac{\psi^{3/2}}{8k^*} < \frac{9c}{32}\sqrt{\psi_i}$$

for all i, which contradicts (2) because $9c/32 < c$. We therefore find that $F(X) \sim \sqrt{\psi}$ as $\psi \to \infty$ when k is chosen appropriately under the Archimedes heuristic with $a = \sqrt{1/\psi}/\pi$. In Section 3 we will use a lower bounding argument to verify that this configuration is in fact optimal, which completes the proof of Claim 2.

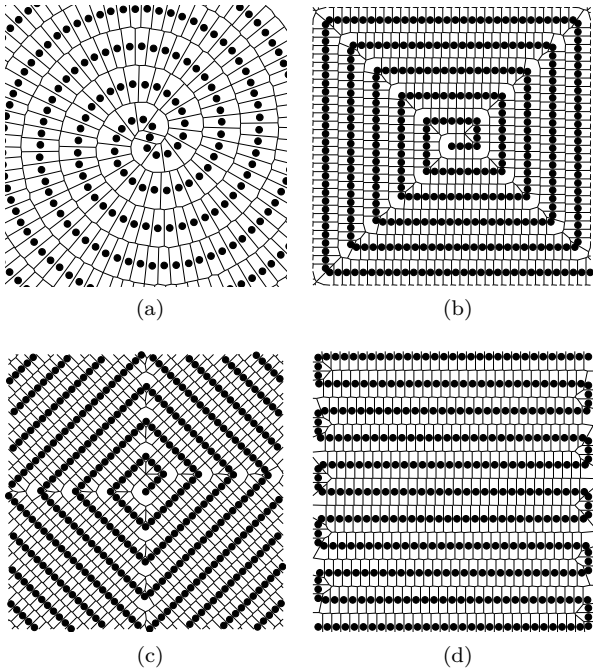

Figure 5: The "double spiral" (5a), facility placement under the square and diamond spirals (5b and 5c), and a "zig-zag" configuration (5d). The key property that these all share is that, like the Archimedes heuristic, we can "unravel" the service region into a long skinny region with dimensions that are actually optimal for the input parameters, as shown in Figure 4.

Remark 3. Using the lower bound in Section 3.2, we can show that Claims 1 and 2 also hold when we use a minimum spanning tree or Steiner tree as our backbone network instead of a TSP tour. For visual purposes, the Archimedes heuristic may appear somewhat unsatisfying due to the terminal endpoint in the center of the region. To work around this, an alternative configuration is the "double spiral" shown in Figure 5a, which inherits the same objective function properties as the single spiral, without this central singularity.

Remark 4. If we assume that the direct transportation cost $\mathrm{Dir}(X, C)$ is taken under the ℓ_1 or ℓ_∞ norm instead of the Euclidean norm, two optimal structures are the square and diamond spirals shown in Figures 5b and 5c. Another possibility would be the "zig-zag" configuration shown in Figure 5d. The key property that all of these configurations share is that we can "unravel" them into a long, skinny region while essentially retaining the same objective value, such as that shown in Figure 4. Since the ℓ_2 norm is rotationally invariant, these configurations are also optimal for our original case where $\mathrm{Dir}(X, C)$ is Euclidean.

Remark 5. The paper [6] considers the problem of minimizing (1) for the special case where $\gamma_k = 0$ for all k and we constrain X to follow either the honeycomb heuristic, a square grid, or an equilateral triangular tiling. The author's analysis is summarized as follows: suppose that k facilities are distributed according to the honeycomb heuristic on a region of area 1. Since the Fermat-Weber value of a hexagon H with unit area is given by

$$\alpha_1 := \mathrm{Dir}\,(H) = \frac{3^{3/4}\,(4 + 3\log 3)\,\sqrt{6}}{108} \approx 0.37721,$$

it is straightforward to see that the Fermat-Weber value of a regular hexagon with area A is $\alpha_1 A^{3/2}$. In our case we have k hexagons with area $1/k$ and therefore the total Fermat-Weber value of our k facilities is simply $k \cdot \alpha_1\,(1/k)^{3/2} = \alpha_1/\sqrt{k}$. Each of these hexagons has sides of length $(\sqrt{2}/3^{3/4}) \cdot (1/\sqrt{k})$ and therefore each point has an associated TSP segment of length $\beta_1/\sqrt{k}$, with $\beta_1 := 3^{-1/4}\sqrt{2} \approx 1.0746$. We therefore find that, as k becomes large, the objective function value

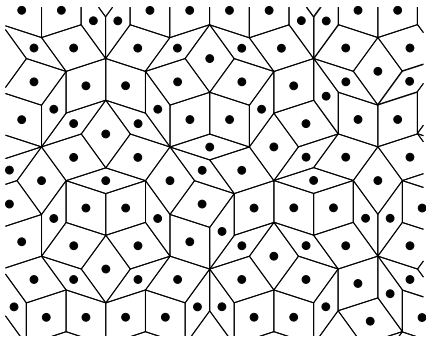

Figure 6: A Penrose tiling of rhombi.

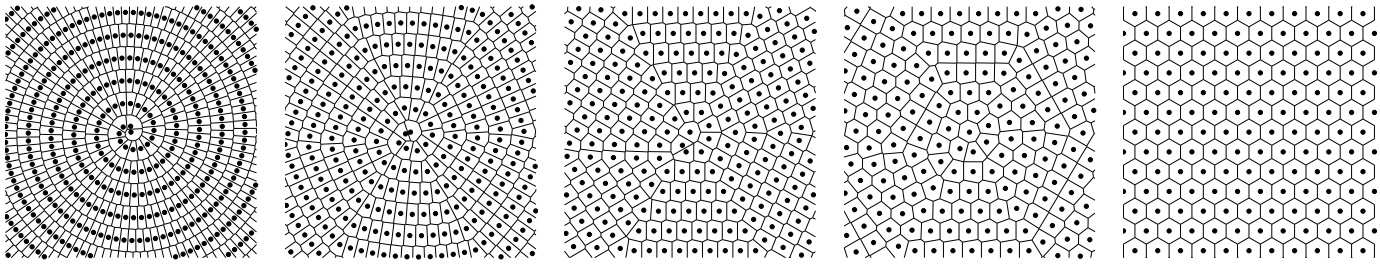

Figure 7: Near-optimal configurations for (1) when $\gamma_k = ck^{-1/2}$, for increasing values of c.

$F(X)$ approaches

$$F(X) \approx (\phi = 1)\beta_1\sqrt{k} + \psi\frac{\alpha_1}{\sqrt{k}}$$

which is minimized at $k = \frac{\psi\alpha_1}{\beta_1}$, at which point the objective function value is

$$2\sqrt{\alpha_1\beta_1\psi} \approx 1.2733\sqrt{\psi}\,. \tag{3}$$

For the square grid, the relevant coefficients (analogous to α_1 and β_1) turn out to be $\alpha_2 \approx 0.38260$ and $\beta_2 = 1$ and for the triangular tiling they are $\alpha_3 \approx 0.40365$ and $\beta_3 \approx 0.87738$. The optimal objective function values for these configurations are $1.2371\sqrt{\psi}$ for the square grid and $1.1902\sqrt{\psi}$ for the triangular layout. Thus, we see that when $\gamma_k \in o(k^{-1/2})$, as $\psi \to \infty$, the Archimedes heuristic out-performs the regular tilings by more than 19%. As an intellectual exercise we may also consider an irregular configuration such as the *Penrose tiling* [16] shown in Figure 6. We find that the relevant coefficients turn out to be $\alpha_4 \approx 0.4560$ and $\beta_4 \approx 0.9578$, giving an optimal objective function value of $1.3217\sqrt{\psi}$.

Remark 6. It is natural to consider the case where $\gamma_k = ck^{-1/2}$ for some constant c, so that neither Claim 1 nor Claim 2 holds. The optimal configuration in such a case ought to depend on the value of c; for very small values of c, a "spiral-like" configuration ought to be near-optimal, and for larger values of c, we expect honeycomb-type configurations to be preferable, as shown in Figure 7.

2.1 Alternative cost models

A gravity model of demand The *gravity hypothesis* [30] is a well-known geographic theory that states that the "interaction" between two points x and y decays at a rate proportional to the inverse square of the distance between them, i.e. $1/\|x-y\|^2$. Here "interaction" might be measured by economic activity [3] or transport [29], for example. We can design a spatial utility model based around the gravity hypothesis by postulating that, if a customer at point x is within the service region of point x_i (i.e. nearer to x_i than any other facility point x_j), then

$$\Pr(\text{customer at } x \text{ uses } x_i) = \frac{1}{(1+\alpha\|x-x_i\|)^2}$$

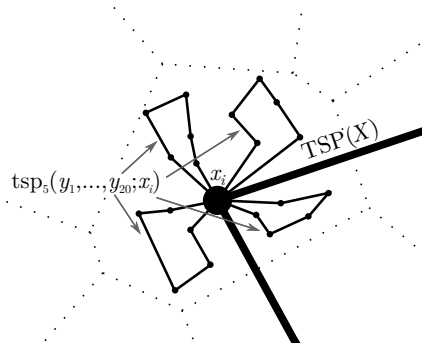

Figure 8: The service region V_i associated with facility x_i and the 4 tours of the "service vehicle" to visit the $N_i = 20$ customers y_i in the region (we have $m = 5$ in this example).

where α is a decay parameter (the "1+" term in the denominator ensures that we have quadratic decay but that the customer uses the facility with probability 1 if $x = x_i$). The total amount of demand served by the facilities X is then proportional to $\tilde{D}(X, C)$, defined as

$$\tilde{D}(X,C) := \iint_C \frac{dA}{(1+\alpha \min_i\{\|x-x_i\|\})^2} = \sum_{i=1}^{k} \iint_{V_i} \frac{dA}{(1+\alpha\|x-x_i\|)^2}$$

where $\mathcal{V} = \{V_1, \ldots, V_k\}$ denotes a Voronoi partition of C with respect to the points X. Since a firm wants $\tilde{D}(X, C)$ to be as large as possible while keeping fixed costs and backbone network costs small, we thus consider the alternative model of (1) given by minimizing

$$\bar{F}(X) = \gamma_{|X|} \cdot |X| + \phi\, \text{TSP}(X) - \psi \tilde{D}(X,C)\,.$$

As in the preceding section, we can analyze the asymptotic behavior of this model when $\psi \to \infty$ by considering the optimal facility placement under the special cases where $\phi = 0$ and $\gamma_k = 0$. Applying a monotonicity argument to that of [18], it is intuitive that when $\phi = 0$, the optimal solution is again the honeycomb heuristic. When $\gamma_k = 0$, the optimal solution is an Archimedean spiral with length $\sqrt{\alpha\psi/2} - \alpha/2 \sim \sqrt{\alpha\psi/2}$. We can easily verify the counterparts to Claims 1 and 2 accordingly.

Multi-trip costs As described in the introduction, the facility-to-customer transportation costs $\psi\,\text{Dir}(X, C)$ model the case where we have a continuum of customers distributed uniformly in C and the cost due to each customer is proportional to the distance between that customer and its nearest facility x_i (a single, direct, round trip between the facility and the customer). We can extend this model to consider the case where a vehicle makes multiple trips to customers, starting and ending at the facility, if we adopt the same assumptions as [26] which are explained below.

More specifically, we suppose that a total of N customers are distributed uniformly in C, and let $\psi' = \psi/N$ so that the transportation costs (when direct trips are used) can equivalently be written as $\psi' N \cdot \text{Dir}(X, C)$; this allows us to describe the transportation costs in terms of the number of customers. In our alternative model, we assume that a service vehicle can visit m customers before a return trip to the facility is required. We let V_i denote the service sub-region (the Voronoi cell) associated with x_i, and suppose that a vehicle based at x_i visits the customers in V_i, of which there are N_i in total. The main assumption of [26] (as stated in the opening paragraph thereof) that we will adopt is that $m \ll N_i$; this simply models the case where there are many required vehicle tours in each sub-region V_i, which might be imposed by lengthy service times at customer locations or limited vehicle capacities (see [7] for a thorough discussion and [5, 17] for probabilistic and worst-case analyses under the same assumptions).

Let $Y = \{y_1, \ldots, y_{N_i}\}$ denote the set of customers distributed in V_i; we will write the cost of servicing the set of customers in V_i as $\text{tsp}_m(Y; x_i)$, where we use the lowercase notation "tsp" to reflect the notion that this travel is happening locally *within* V_i, as opposed to the backbone network costs $\text{TSP}(X)$ which occur between facilities; see Figure 8. Each vehicle's route will consist of at most $m + 1$ stops, namely, a set of m customers plus the starting point x_i; the original case where transportation costs are $\psi\,\text{Dir}(X, C)$ is simply the special case of this new formulation in which $m = 1$.

Since we assume that the customers are distributed uniformly at random in V_i, we define

$$\mathrm{Etsp}_m(V_i, x_i) = \mathbf{E}\,\mathrm{tsp}_m(Y; x_i)$$

as the expected distance that the vehicle serving region V_i will traverse. The total expected transportation cost to customers is then given by $(\psi'/2)\,\mathrm{Etsp}_m(V_i, x_i)$, where we have used a coefficient $\psi'/2$ rather than ψ' because of the implicit multiplier "2" that we introduced when we defined ψ in Table 1. The purpose of this multiplier was to account for the inbound and outbound components of travel (which we no longer have to consider in such a fashion in the multi-stop model). Theorem 4 of [17] then says that, provided m is fixed, we have

$$\mathrm{Etsp}_m(V_i, x_i) \sim \frac{2N_i}{m} \cdot \frac{\iint_{V_i} \|x - x_i\|\, dA}{\mathrm{Area}(V_i)}$$

as $N_i \to \infty$. The survey [5] provides an intuitive justification for this relationship in the following passage, where we have replaced some of the original notation with our own for the sake of consistency:

> Any solution for the capacitated VRP has two cost components; the first component is proportional to the total "radial" cost between the depot and the customers. The second component is proportional to the "circular" cost; the cost of traveling between customers. This cost is related to the cost of the optimal traveling salesman tour. It is well known [2] that, for large N_i, the cost of the optimal traveling salesman tour grows like $\sqrt{N_i}$, while the total radial cost between the depot and the customers grows like N_i because the number of vehicles used in any solution is at least $\lceil N_i/m \rceil$. Therefore, it is intuitive that when the number of customers is large enough the first cost component will dominate the optimal solution value.

Returning to our problem, we see that since $N_i \sim N \cdot \mathrm{Area}(V_i)$ as $N \to \infty$ (with probability 1), it must follow that the total transportation cost in the region is then

$$\begin{aligned}
\sum_{i=1}^{k} (\psi'/2)\,\mathrm{Etsp}_m(V_i, x_i) &\sim \sum_{i=1}^{k} (\psi'/2) \left(\frac{2N_i}{m} \cdot \frac{\iint_{V_i} \|x - x_i\|\, dA}{\mathrm{Area}(V_i)} \right) \\
&\sim \sum_{i=1}^{k} \frac{\psi' \cdot N}{m} \iint_{V_i} \|x - x_i\|\, dA = \frac{\psi}{m}\,\mathrm{Dir}(X, C)
\end{aligned}$$

which differs from the transportation cost in our initial formulation merely by a factor of $1/m$. Thus, we find that the introduction of a multi-stop model for transportation cost within sub-regions does not alter our model in a fundamental way, provided that the number of stops allowed on a vehicle tour, m, is small relative to the total number of clients in each sub-region, N_i.

Competition with backbone network costs One might also view the preceding result within the context of competitive location problems, in which the objective is to find the best location for a new facility in order to attract the most buying power away from existing facilities, and conversely to determine the optimal location for the "defending" facilities in order to minimize the attractive power of the new facility. When the number of facilities is fixed and $\phi = 0$, the honeycomb heuristic is currently the best-known "defensive" configuration for facilities in the plane, and in [13] it is shown that it is within 2.5% of a lower bound for the optimal such solution.

Another variation would be the problem of constructing a "defensive" configuration of facilities that also takes into account the cost of the backbone network. We can write this problem as

$$\underset{X}{\text{minimize}}\ \gamma_{|X|} \cdot |X| + (\phi = 1)\,\mathrm{TSP}(X) + \psi \max_{p \in C} S(p\,|X\,) \tag{4}$$

where $S(p\,|X\,)$ denotes the amount of area that "attacking" facility p "steals" from the facilities X (see Figure 9). From [13] we have bounds for $S(p\,|X\,)$ for the square grid, triangular tiling, and honeycomb heuristic, which are reproduced in Table 2.[2] Using the values ζ_i as in the table, and re-introducing the values β_i from earlier (the "TSP coefficients"), we

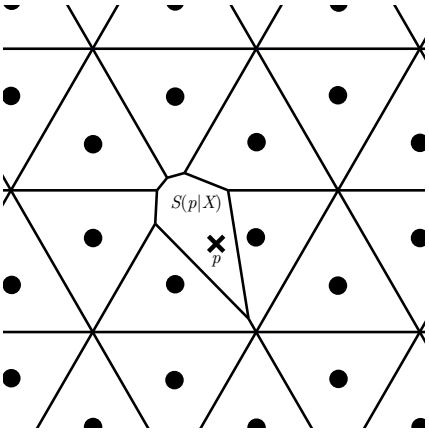

Figure 9: Competitive placement of a facility p where "defending" facilities are distributed in a triangular tiling; the above placement of p is sub-optimal.

Configuration	Constant	Upper bound
Honeycomb	ζ_1	0.5127
Square	ζ_2	0.5625
Triangular	ζ_3	2/3

Table 2: Upper bounds for $S(p\,|X\,)$, the amount of area that an "attacking" facility p can "steal" from the "defending" facilities X. The values ζ_i are defined as follows: if $|X| = k$ and $\text{Area}(C) = 1$, then each facility's service region (Voronoi cell) will have area $1/k$. An attacking facility can "steal" at most ζ_i/k from X; in other words, ζ_i represents the amount of area that an attacking facility can steal, measured as a fraction of the area of any defending facility's service region.

find that our objective can be written as

$$\underset{k}{\text{minimize}}\ \gamma_k \cdot k + (\phi = 1)\beta_i\sqrt{k} + \psi\zeta_i/k$$

whose asymptotic behavior we will again analyze in terms of $\{\gamma_k\}$ as $\psi \to \infty$. As before, it is obvious that if $\gamma_k \in \omega(k^{-1/2})$, then the fixed costs dwarf the backbone network costs as $\psi \to \infty$ (since $k \to \infty$ also), and the honeycomb heuristic is therefore asymptotically optimal (assuming that the honeycomb heuristic is indeed the optimal competitive configuration when there is no backbone network cost, as conjectured in [13]).

The case where $\gamma_k \in o(k^{-1/2})$ is slightly more involved. If we consider the problem where fixed costs are omitted, i.e.

$$\underset{X}{\text{minimize}}\ (\phi = 1)\,\text{TSP}(X) + \psi \max_{p \in C} S(p\,|X\,),$$

then we find that optimal objective value is $(3 \cdot 2^{1/3}/2)\beta_i^{2/3}\psi^{1/3}\zeta_i^{1/3}$ for each of the regular tilings, namely $1.587\psi^{1/3}$ for the honeycomb placement, $1.560\psi^{1/3}$ for the square grid, and $1.513\psi^{1/3}$ for the triangular layout. This is because we can write the problem as

$$\underset{X}{\text{minimize}}\ (\phi = 1)\beta_i\sqrt{k} + \psi\zeta_i/k$$

and subsequently solve for the optimal k.

However, if we place an infinite number of facilities together along an Archimedean spiral of length ℓ, then as Figure 10 shows, the maximum area that the attacker p can "steal" from the defending facilities X, $S(p\,|X\,)$, is approximately $1/3\ell^2$. Thus we consider the problem

$$\underset{\ell}{\text{minimize}}(\phi = 1)\ell + \frac{\psi}{3\ell^2}$$

which has an optimal solution $\ell^* = 18^{1/3}\psi^{1/3}/3$, at which point the objective value is $c\psi^{1/3}$, where $c = 18^{1/3}/2 \approx 1.310$. We conjecture that the Archimedean spiral is an optimally competitive configuration for this problem, although a rigorous

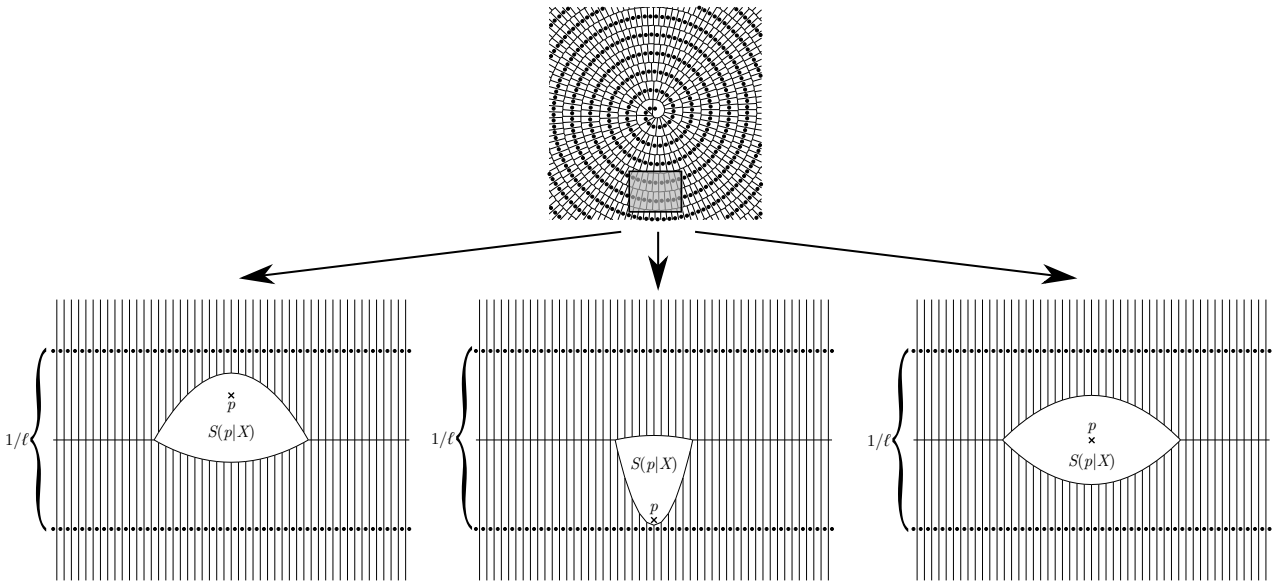

Figure 10: Three possible locations for the attacking facility against the Archimedes configuration. Not surprisingly, the third location (exactly between the two arcs of the spiral) maximizes the amount of area that the attacking facility can steal.

proof appears difficult. In Section B of the online supplement, we show that if $\gamma_k \in o(k^{-1/2})$, then the optimal objective function cost is $c\psi^{1/3} + o(\psi^{1/3})$.

3 Lower bounds in a convex region

In this section we introduce some lower bounds for the objective function $F(X)$ defined on a given convex region C. We begin with a collection of bounds relating $\mathrm{Dir}(X, C)$, $\mathrm{TSP}(X)$, and $|X| = k$.

3.1 Bounds for $\mathrm{Dir}(X, C)$ and $\mathrm{TSP}(X)$

Lemma 7. *For any region C with area A, we have*

$$\mathrm{Dir}\,(C) \geq \frac{2A^{3/2}}{3\sqrt{\pi}}\,.$$

Proof. It is well-known that, for a fixed area A, a disk with radius $\sqrt{A/\pi}$ is the region with minimal Fermat-Weber value. The above expression is merely the Fermat-Weber value of such a disk. □

Corollary 8. *For any region C with area A containing a set of points $X = \{x_1, \ldots, x_k\}$, we have $\mathrm{Dir}(X, C) \geq {}^{2A^{3/2}}/_{3\sqrt{\pi k}}$.*

Theorem 9. *Suppose that $X = \{x_1, \ldots, x_k\}$ is a set of points in a convex polygon C such that $\mathrm{TSP}\,(X) = \ell$ and $\mathrm{Area}(C) = A$. Then $\mathrm{Dir}\,(X, C) \geq {}^{2A^{3/2}}/_{3\sqrt{\pi k}}$ and $\mathrm{Dir}\,(X, C) \geq \frac{2A^2}{8\ell + 3\sqrt{\pi A}}$.*

Proof. The first inequality follows from Lemma 7. The second follows via two simple lemmas, which we will now prove. We first make the observation that if P is a TSP tour of the points X, then obviously $\mathrm{Dir}(X, C) \geq \mathrm{Dir}(P, C)$ (since $X \subset P$), and therefore we can consider bounding the quantity $\mathrm{Dir}(P, C)$ over all paths with a given length ℓ.

Lemma 10. *For any path P of length ℓ and any ϵ, we have $\mathrm{Area}\,(N_\epsilon\,(P)) \leq \pi\epsilon^2 + 2\epsilon\ell$, which is tight when P is a line segment.*

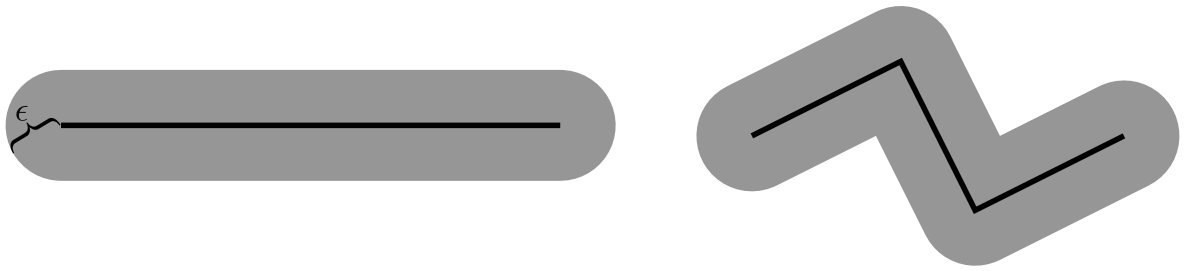

(a) (b)

Figure 11: The neighborhoods $N_\epsilon(P)$ for two paths of the same length, a line segment (11a) and a collection of segments (11b).

Proof. Note this lemma applies to *all* paths, and not merely those that are closed (that would be the most appropriate setting for TSP tours, although the analysis thereof appears difficult). We prove this by induction on the number of line segments n that comprise P. The base case $n = 1$ is simply a line segment for which $N_\epsilon(P)$ is shown in Figure 11a. To complete the induction, consider a path consisting of n line segments, which we can think of as the union of a path $P^{'}$ with length $\ell^{'}$ with $n-1$ line segments, and a line segment s of length $\ell^{''}$ such that $\ell = \ell^{'} + \ell^{''}$. Let $P^{'} \cup s = P$ denote their union. Since $P^{'}$ and s are joined at a point, the neighborhoods $N_\epsilon(P^{'})$ and $N_\epsilon(s)$ must both contain a ball of radius ϵ about their point of intersection; in other words, we have $\text{Area}(N_\epsilon(P^{'}) \cap N_\epsilon(s)) \geq \pi\epsilon^2$ and therefore we find that

$$\begin{aligned} \text{Area}(N_\epsilon(P)) &= \text{Area}(N_\epsilon(P^{'} \cup s)) = \text{Area}(N_\epsilon(P^{'}) \cup N_\epsilon(s)) \\ &= \underbrace{\text{Area}(N_\epsilon(P^{'}))}_{\leq \pi\epsilon^2 + 2\epsilon\ell^{'}} + \underbrace{\text{Area}(N_\epsilon(s))}_{\leq \pi\epsilon^2 + 2\epsilon\ell^{''}} - \underbrace{\text{Area}(N_\epsilon(P^{'}) \cap N_\epsilon(s))}_{\geq \pi\epsilon^2} \end{aligned}$$

and the desired result follows. □

Lemma 11. *Let P denote a path with length ℓ and let C denote a planar region with area A containing P. Further let L denote a line segment with length ℓ and let $\epsilon_L^{\max}$ be chosen so that $\text{Area}(N_{\epsilon_L^{\max}}(L)) = A$. Then $\text{Dir}(L, N_{\epsilon_L^{\max}}(L)) \leq \text{Dir}(P, C)$; in other words, for a given area A, among all paths with fixed length ℓ, a line segment and its appropriately-chosen neighborhood have the minimal Fermat-Weber value.*

Proof. Assume without loss of generality that $A = 1$ and let $\epsilon_P^{\max}$ be chosen so that $\text{Area}(N_{\epsilon_P^{\max}}(P)) = A = 1$. It is obvious that $\text{Dir}(P, N_{\epsilon_P^{\max}}(P)) \leq \text{Dir}(P, C)$ for all regions C with area 1. Thus it will suffice to show that $\text{Dir}(P, N_{\epsilon_P^{\max}}(P)) \geq \text{Dir}(L, N_{\epsilon_L^{\max}}(L))$. Consider a random variable ϵ_P defined by setting $\epsilon_P := D(z, P)$, where z is a random variable sampled uniformly from $N_{\epsilon_P^{\max}}(P)$, and define ϵ_L similarly. Note that the cumulative distribution functions for ϵ_P and ϵ_L are given by

$$\begin{aligned} F_P(\epsilon_P) &= \min\{1, \text{Area}(N_{\epsilon_P}(P))\} \\ F_L(\epsilon_L) &= \min\{1, \text{Area}(N_{\epsilon_L}(L))\}\,. \end{aligned}$$

By Lemma 10, for any $\epsilon > 0$, we have $F_L(\epsilon) \geq F_P(\epsilon)$. Next note that

$$\mathbf{E}(\epsilon_L) = \int_0^\infty 1 - F_L(\epsilon)\, d\epsilon \leq \int_0^\infty 1 - F_P(\epsilon)\, d\epsilon = \mathbf{E}(\epsilon_P)\,,$$

a well-known result of first-order stochastic dominance (see page 249 of [27], for instance). The proof is complete by observing that by definition, $\mathbf{E}(\epsilon_L) = \text{Dir}(L, N_{\epsilon_L}(L))$ and $\mathbf{E}(\epsilon_P) = \text{Dir}(P, N_{\epsilon_P}(P))$. □

Having established the two preceding lemmas, we next note that for any line segment L with length ℓ and any ϵ, we can compute

$$\begin{aligned} \text{Area}(N_\epsilon(L)) &= \pi\epsilon^2 + 2\epsilon\ell \qquad (5) \\ \text{Dir}(L, N_\epsilon(L)) &= \frac{2\pi\epsilon^3}{3} + \epsilon^2\ell\,. \end{aligned}$$

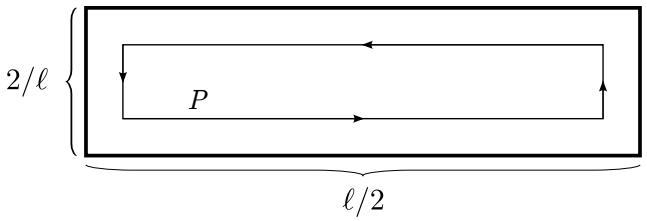

Figure 12: When C is the rectangle shown above and P is the path indicated, we find that as $\ell \to \infty$, we have $\mathrm{Dir}(P, C) \sim 1/4\ell$ so that the second lower bound of Theorem 9 becomes tight.

Solving equation (5) in terms of $\epsilon > 0$ and substituting, we find that

$$\mathrm{Dir}(L, N_\epsilon(L)) = \frac{-2\ell^3 - 3\pi\ell\,\mathrm{Area}(N_\epsilon(L)) + (2\ell^2 + 2\pi\,\mathrm{Area}(N_\epsilon(L)))\sqrt{\ell^2 + \pi\,\mathrm{Area}(N_\epsilon(L))}}{3\pi^2} \geq \frac{2A^2}{8\ell + 3\sqrt{\pi A}},$$

where $A = \mathrm{Area}(N_\epsilon(L))$ (we have performed some routine calculations in the inequality above which we omit for brevity).

Our proof of Theorem 9 is complete; if we let P be a TSP tour of any point set X, contained in a region C with area A, then

$$\mathrm{Dir}(X, C) \geq \mathrm{Dir}(P, C) \geq \mathrm{Dir}(P, N_{\epsilon_P^{\max}}(P)) \geq \mathrm{Dir}(L, N_{\epsilon_L^{\max}}(L)) \geq \frac{2A^2}{8\ell + 3\sqrt{\pi A}}$$

where $\mathrm{length}(P) = \mathrm{length}(L)$ and $\epsilon_P^{\max}$ and $\epsilon_L^{\max}$ are chosen so as to induce the appropriate areas. □

The second bound of Theorem 9 is useful because it establishes the inverse proportionality between the backbone linehaul network length $\ell = \mathrm{TSP}(X)$ and the transportation cost to customers, $\mathrm{Dir}(X, C)$. More broadly, one could use this result to understand the best possible marginal improvement to local transportation $\mathrm{Dir}(X, C)$ one could obtain by lengthening the backbone network.

Remark 12. In addition to giving us a lower bound, Theorem 9 also suggests what kind of *region* ought to be efficient for our original problem: consider a rectangle of dimensions $(\ell/2) \times (2/\ell)$ containing a path P of length ℓ as shown in Figure 12. It is not hard to verify that $\mathrm{Dir}(P, C) \sim 1/4\ell$ as $\ell \to \infty$, so that the second bound of Theorem 9 becomes tight. This equivalently suggests that such regions ought to be optimal for instances of our original problem (1), much in the same spirit as the design of "zones" in Figure 2 of [26].

Before describing our approximation algorithm, we must introduce an additional lower bound which applies when C is a particularly long, skinny region. To quantify this, we orient C so that $\mathrm{diam}(C)$ is aligned with the coordinate x-axis, and we assume without loss of generality that C is contained in a box of dimensions $(\mathrm{diam}(C) = w) \times h$, where $w \geq h$. By convexity of C it immediately follows that

$$wh/2 \leq \mathrm{Area}(C) \leq wh\,.$$

Lemma 13. *For any region C with area A contained between two lines a distance h apart, we have* $\mathrm{Dir}(C) \geq A^2/4h$.

Proof. Assume without loss of generality that the two lines in question are horizontal and consider any point $x_0 = (x_1^0, x_2^0)$ between them. Clearly for any point $x = (x_1, x_2)$ we have $\|x_0 - x\| \geq |x_1^0 - x_1|$. It is easy to see that the region that minimizes $\iint_C |x_1^0 - x_1|\,dA$ (subject to the constraint that C be contained between the two lines) is simply a rectangle with height h and width A/h. The value $\iint_C |x_1^0 - x_1|\,dA$, which is a lower bound on the Fermat-Weber value of such a rectangle, is precisely $\int_0^h \int_{-A/(2h)}^{A/(2h)} |x|\,dx\,dy = \frac{A^2}{4h}$ as desired. □

Theorem 14. *Suppose that $X = \{x_1, \ldots, x_k\}$ is a set of points in a convex polygon C such that* $\mathrm{TSP}(X) = \ell < A/h$. *Then* $\mathrm{Dir}(X, C) \geq A^2/4hk$ *and* $\mathrm{Dir}(X, C) \geq (A - h\ell)^2/4h$.

Proof. The first inequality follows immediately from Lemma 13. Assume without loss of generality that $x_1 = (x_1^1, x_2^1)$ is the leftmost point in X and $x_k = (x_1^k, x_2^k)$ is the rightmost point in X. Clearly $x_1^k - x_1^1 \leq \ell/2$ since a TSP tour must

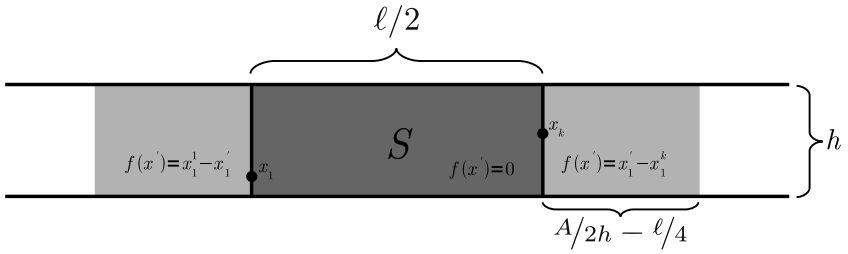

Figure 13: The distribution of area that minimizes $f(x')$.

return to its starting point. The maximum amount of area of C that can be contained in the slab S between the lines $\ell_1 = \{(x_1, x_2) : x_1 = x_1^1\}$ and $\ell_2 = \{(x_1, x_2) : x_1 = x_1^k\}$ is $h\ell/2$. Thus, we have at least $A - h\ell/2$ units of area of C remaining to distribute outside S. Let $x' = (x_1', x_2')$ be a dummy variable and consider the function $f(x')$ defined by

$$f(x') = \begin{cases} x_1^1 - x_1' & \text{if } x_1' \leq x_1^1 \\ 0 & \text{if } x_1^1 < x_1' < x_1^k \\ x_1' - x_1^k & \text{otherwise} \end{cases}$$

and note that clearly $f(x') \leq \min_{x_i \in X} \|x' - x_i\|$. We now consider the problem of distributing the remaining $A - h\ell/2$ units of area in the rectangle so as to minimize the integral of $f(x')$. The obvious solution is to distribute $A/2 - h\ell/4$ units of area to the right and to the left of S in rectangles of dimensions $A/2h - \ell/4 \times h$ as shown in Figure 13. The integral of $f(x')$ over this shape is precisely $\frac{(A-h\ell/2)^2}{4h}$ as desired. □

3.2 Minimizing $F(X)$

Having proven Theorems 9 and 14, we can derive lower bounds on the objective function $F(X)$ of (1) by solving the following optimization problems, where we let ℓ and z denote variables corresponding to $\mathrm{TSP}(X)$ and $\mathrm{Dir}(X, C)$, and we assume (for now) that $k = |X|$ is fixed:

$$\begin{aligned} \underset{\ell,z}{\text{minimize}}\ \gamma_k \cdot k + \phi\ell + \psi z \qquad & s.t. \\ z &\geq \frac{2A^{3/2}}{3\sqrt{\pi k}} \\ z &\geq \frac{2A^2}{8\ell + 3\sqrt{\pi A}} \\ z, \ell &\geq 0 \end{aligned} \tag{6}$$

$$\begin{aligned} \underset{\ell,z}{\text{minimize}}\ \gamma_k \cdot k + \phi\ell + \psi z \qquad & s.t. \\ z &\geq \frac{A^2}{4hk} \\ z &\geq \frac{(A - h\ell/2)^2}{4h} \mathbb{1}(\ell/2 < A/h) \\ z, \ell &\geq 0\,. \end{aligned} \tag{7}$$

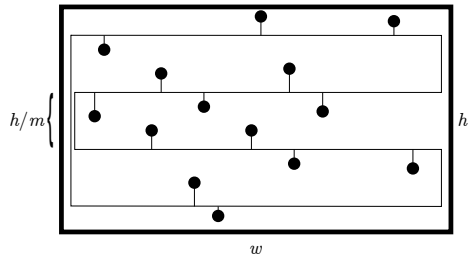

Figure 14: The TSP path construction that satisfies (11), here with $m = 4$.

Here $\mathbb{1}(\cdot)$ denotes the indicator function. It is easy to show that the optimal objective function value to (6) is

$$\Phi^1_{\mathrm{LB}}(A,\phi,\psi,k) = \gamma_k \cdot k + \begin{cases} \frac{3\sqrt{A\pi}}{8}(\sqrt{k/\psi}-1)\phi + \frac{2A^{3/2}\psi^{3/2}}{3\sqrt{\pi k}} & \text{if } \phi \le \frac{16A\psi^2}{9\pi k} \\ A\sqrt{\phi\psi} - \frac{3\phi\sqrt{\pi A}}{8} & \text{if } \frac{16A\psi^2}{9\pi k} < \phi \le \frac{16A\psi}{9\pi} \\ \frac{2\psi A^{3/2}}{3\sqrt{\pi}} & \text{otherwise} \end{cases} \tag{8}$$

and the optimal objective function value to (7) is

$$\Phi^2_{\mathrm{LB}}(A,\phi,\psi,h,k) = \gamma_k \cdot k + \begin{cases} \frac{2(1+1/\sqrt{k})A}{h}\phi + \frac{A^2}{4hk}\psi & \text{if } \phi \le \frac{A\psi}{4\sqrt{k}} \\ \frac{2\phi A}{h} - \frac{4\phi^2}{\psi h} & \text{if } \frac{A\psi}{4\sqrt{k}} < \phi \le \frac{A\psi}{4} \\ \frac{A^2}{4h}\psi & \text{otherwise} \end{cases} \tag{9}$$

and therefore a lower bound for our objective function (1) is

$$\Phi_{\mathrm{LB}}(A,\phi,\psi,h,k) = \max\{\Phi^1_{\mathrm{LB}}(A,\phi,\psi,k)\,,\,\Phi^2_{\mathrm{LB}}(A,\phi,\psi,h,k)\}\,. \tag{10}$$

Note that the second case of Φ^1_{LB} can be used to prove that the Archimedes heuristic is asymptotically optimal as $\psi \to \infty$ (for the case where $\gamma_k \in o(k^{-1/2})$), since we have $\Phi^1_{\mathrm{LB}} \sim \sqrt{\psi}$ when $A = 1$, $\phi = 1$, and ψ and k become large as in Section 2.

4 Upper bounds in a convex region

In this section we give some upper bounds for $\mathrm{TSP}(X)$ and $\mathrm{Dir}(X, C)$ which we will use in proving that our algorithm produces a solution within a constant factor of optimality.

Theorem 15. *Suppose that $X = \{x_1, \ldots, x_k\}$ is a set of points distributed in a rectangle R having dimensions $w \times h$. For any positive even integer m, we have*

$$\mathrm{TSP}(X) \le G(w,h,k) := hk/m + mw + 2\left(\frac{m-1}{m}\right)h\,. \tag{11}$$

Proof. This is due to [14]. We will show how to construct a path through the points X whose length is bounded by the above quantity. One way to form such a path is to move along R horizontally m times, making vertical diversions to touch each of the points, as shown in Figure 14. It is easy to see that if we ignore the additional work needed to visit the points X, the length of the path is $mw + 2\frac{m-1}{m}h$. The distance from each point x_i to the main path is at most $h/2m$ and therefore each such point introduces no more than h/m additional work to the path, which gives the desired result. □

Remark 16. Note that as $hk/w \to \infty$, by setting $m = 2 \cdot \lfloor\sqrt{hk/w}/2\rceil$, we find that $G(w,h,k) \sim 2\sqrt{whk}$. This proportionality to $\sqrt{k}$ is consistent with well-known results in geometric probability such as [28, 31]. A more precise discussion of path constructions of these types can be found in [11].

We can now define a function $H(A, w, h)$, which is an upper bound on the Fermat-Weber value of a convex region with area A contained in a box of dimensions $w \times h$, assuming that $w \geq h$:

Theorem 17. *Suppose that C is a convex region with area A in a rectangle R having dimensions $w \times h$, with $w \geq h$. We have*

$$\mathrm{Dir}(C) \leq H(A, w, h) := \begin{cases} \left[\log\left(\frac{h+\sqrt{w^2+h^2}}{wa+w\sqrt{1+a^2}}\right) - a\sqrt{1+a^2}\right]\frac{w^3}{12} + \left[\log\left(\frac{bw+b\sqrt{w^2+h^2}}{h+h\sqrt{b^2+1}}\right) - \frac{\sqrt{b^2+1}}{b^2}\right]\frac{h^3}{12} + \frac{wh\sqrt{w^2+h^2}}{6} & \text{if } A < wh - \frac{h}{2}\sqrt{w^2-h^2} \\ \log\left(\frac{h+\sqrt{w^2+h^2}}{w}\right)\cdot\frac{w^3}{12} + \left[\log\left(\frac{cw+c\sqrt{w^2+h^2}}{h+h\sqrt{c^2+1}}\right) - \frac{\sqrt{1+c^2}}{c^2}\right]\frac{h^3}{12} + \frac{1}{6}wh\sqrt{w^2+h^2} & \text{otherwise}, \end{cases}$$

where

$$\begin{aligned} a &= \frac{w^3h - wh^3 - 2(wh-A)\sqrt{(w^2+h^2)^2 - 8hwA + 4A^2}}{2Awh - 2w^2h^2 - w^2\sqrt{(w^2+h^2)^2 - 8hwA + 4A^2}} \\ b &= \frac{2(wh^3 - Ah^2) + wh\sqrt{h^4 + 2w^2h^2 + w^4 - 8Awh + 4A^2}}{w^4 + 3w^2h^2 - 8Awh + 4A^2} \\ c &= \frac{h^2}{2(wh-A)}. \end{aligned}$$

Proof. See Section C of the online supplement. □

Remark 18. It is not hard to show that, if we fix the product wh, then as $h/w \to 0$, we have

$$H(A, w, h) \sim \frac{2}{3}Aw - \frac{1}{12}w^2h - \frac{1}{3}\cdot\frac{A^2}{h} \tag{12}$$

for all A (see Section C of the online supplement). It can also be shown that, for fixed w and h, the function $H(A, w, h)$ is concave in A.

5 An approximation algorithm

In this section we describe our simple algorithm for placing facilities in C so as to (approximately) minimize the objective function of (1). In the asymptotic analysis, we assumed (without loss of generality) that $\phi = 1$ and that $A = 1$; in this section, we shall assume that $\psi = 1$ so that ϕ is allowed to vary instead (this simplifies some of the notation and limits the use of fractions somewhat). Thus, the input to our algorithm is a convex polygon C, a scalar ϕ, and a sequence $\{\gamma_k\}$ such that $\gamma_k \cdot k$ is increasing. We first describe a subroutine that constructs, for any given integer k, an approximately optimal placement of k facilities; we then apply this subroutine with strategic values of k so as to produce an overall approximation guarantee.

Assume that C is aligned so that its diameter coincides with the coordinate x-axis. We then enclose C in an axis-aligned box $\square C$ of dimensions $w \times h$, where we assume without loss of generality that $w = 1/h = \mathrm{diam}\,(C)$; convexity of C immediately implies that $A = \mathrm{Area}(C) \in [1/2, 1]$. In our algorithm, we then let $k_1 = \lfloor k/2 \rfloor$ and $k_2 = \lceil k/2 \rceil$ and divide $\square C$ into two pieces of areas $(k_1/k)\cdot\mathrm{Area}\,(\square C) = k_1/k$ and $(k_2/k)\cdot\mathrm{Area}\,(\square C) = k_2/k$ respectively, using a vertical line. This is performed recursively (with the option to split using a horizontal line, if the height of an intermediate sub-region exceeds its width) until all regions have area $1/k$. This is described in Algorithms 1 and 2 and Figures 15 and 16. As an aside, it turns out that Algorithm 2 is a constant-factor approximation algorithm for the continuous k-medians problem in a convex polygon (that is, minimizing $\mathrm{Dir}\,(X, C)$ in a given convex polygon C with a constraint that $|X| = k$), with approximation constant 2.74 [10].

Definition 19. The *aspect ratio* of a rectangle R, written $\mathrm{AR}(R)$, is the ratio of the longer side of R to the shorter side.

Before defining the appropriate values of k that should be passed to Algorithm 2 to solve our problem, we state the following claim:

Claim 20. Suppose that $\square C$ is a box of dimensions $w \times h$, where $w \geq h$, and that $R_1, \ldots, R_k$ is the output of Algorithm 1. If $k \geq w/3h$, then we have $\mathrm{AR}(R_i) \leq 3$ for all rectangles R_i. If $k < w/3h$, then $\mathrm{AR}(R_i) = w/hk$.

Input: An axis-aligned rectangle R and an integer k.
Output: A partition of R into k rectangles, each having area $\text{Area}(R)/k$.
if $k = 1$ **then**
  return R;
else
  Set $k_1 = \lfloor k/2 \rfloor$ and $k_2 = \lceil k/2 \rceil$;
  Let w denote the width of R and h the height; **if** $w \geq h$ **then**
    With a vertical line, divide R into two pieces R_1 and R_2 with area $\frac{k_1}{k} \cdot \text{Area}(R)$ on the right and $\frac{k_2}{k} \cdot \text{Area}(R)$ on the left;
  else
    With a horizontal line, divide R into two pieces R_1 and R_2 with area $\frac{k_1}{k} \cdot \text{Area}(R)$ on the top and $\frac{k_2}{k} \cdot \text{Area}(R)$ on the bottom;
  end
  return $\mathit{RectanglePartition}(R_1, k_1) \cup \mathit{RectanglePartition}(R_2, k_2)$;
end

Algorithm 1: Algorithm $\text{RectanglePartition}(R, k)$ takes as input an axis-aligned rectangle R and a positive integer k. This is used as a subroutine in Algorithm 2.

Input: A convex polygon C and an integer k.
Output: The locations of k points p_i in C that approximately minimize $\text{Dir}(C, k)$ within a factor of 2.74.
Align a diameter of C with the coordinate x-axis;
Let $\square C$ denote an axis-aligned box of dimensions $w \times h$, where $w = \text{diam}(C)$;
Let $R_1, \ldots, R_k = \text{RectanglePartition}(\square C, k)$;
for $i \in \{1, \ldots, k\}$ **do**
  Let c_i denote the center of R_i;
  if $c_i \in C$ **then**
    Set $p_i = c_i$;
  else
    if $R_i \cap C$ *is nonempty* **then**
      Let $R_i^{'}$ be the minimum axis-aligned bounding box of $R_i \cap C$ and let $c_i^{'}$ denote its center;
      Set $p_i = c_i^{'}$;
    else
      Place p_i anywhere in C;
    end
  end
end
return $p_1, \ldots, p_k$;

Algorithm 2: Algorithm $\text{ApproxFW}(C, k)$ takes as input a convex polygon C and an integer k.

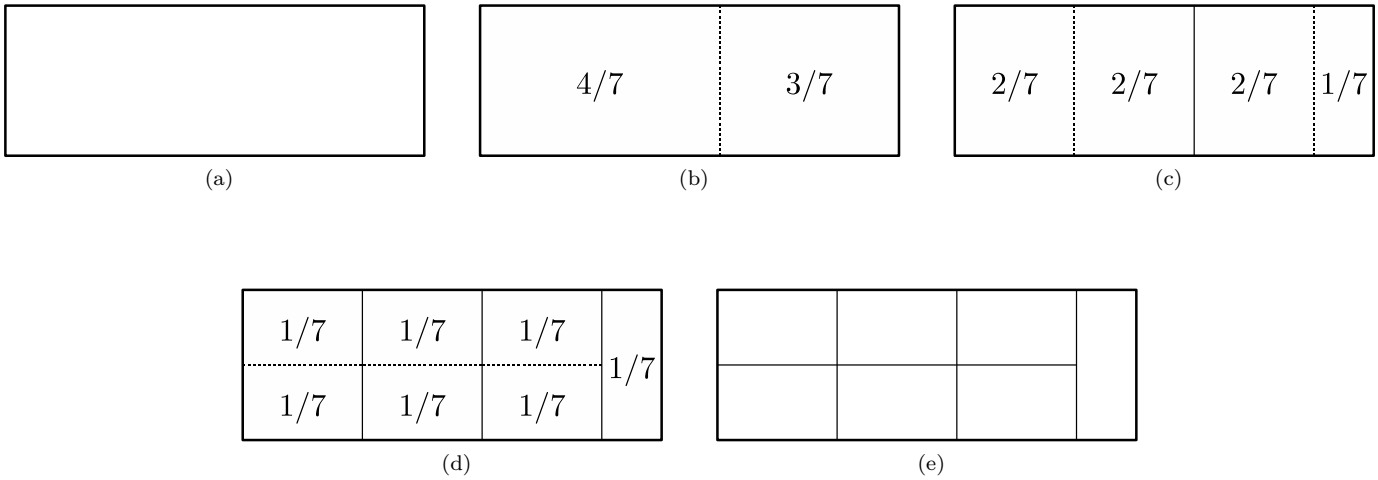

Figure 15: The input and output of Algorithm 1. We begin in (15a) with a rectangle R and an integer $k = 7$; here we assume that $\text{Area}(R) = 1$. In Figures (15b) through (15d), we subdivide R into smaller rectangles by a recursive subdivision; the areas of each sub-rectangle are shown. Figure (15e) shows the output.

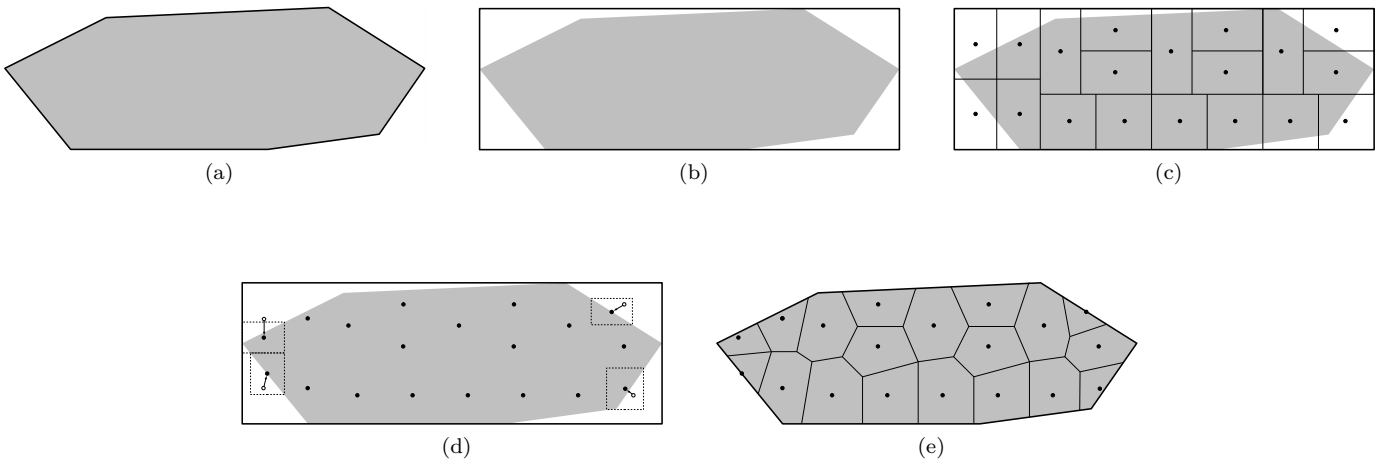

Figure 16: The input and output of Algorithm 2. We begin in (16a) with a convex polygon C, whose axis-aligned bounding box $\square C$ is computed in (16b). The bounding box is then partitioned into $k = 19$ equal-area pieces in (16c) using Algorithm 1. Some of the centers of these pieces are then relocated in (16d), and (16e) shows the output and Voronoi partition.

Proof. This is straightforward and explained in Section D of the online supplement. □

Using the preceding results we can now present our approximation algorithm for placing facilities so as to minimize (1), which is given in Algorithm 3. In the following section we will prove that this is a constant-factor approximation algorithm.

Input: A convex polygon C with area $A \in [1/2, 1]$ contained in a minimum bounding box of dimensions $(\text{diam}(C) = 1/h = w) \times h$, a positive scalar ϕ, and a sequence γ_k such that $\gamma_k \cdot k$ is increasing.
Output: The locations of a finite set of points X in C that approximately minimize $F(X) = \gamma_{|X|} \cdot |X| + \phi\,\text{TSP}\,(X) + \text{Dir}\,(X, C)$ within a factor of 3.93.
Let $\alpha := H\left(A, \sqrt{3}, 1/\sqrt{3}\right)$ and $K := \max\left\{\left\lfloor \frac{\alpha}{2\phi} \right\rceil, \lfloor \frac{1}{h^2} \rceil\right\}$;
Set $v^* = \infty$;
for $k \in \{1, \ldots, K\}$ **do**
  Let $X = \text{ApproxFW}(C, K)$;
  if $F(X) \leq v^*$ **then**
    Set $v^* := F(X)$ and $X^* := X$;
  end
end
return X^*;

Algorithm 3: Algorithm FacilityPlacement(C, ϕ, γ_k) takes as input a convex polygon C, a sequence γ_k, and a positive scalar ϕ.

6 Proof of approximation bounds

In this section we show that Algorithm 3 produces a constant-factor approximation for the problem of minimizing the function $f(X)$ defined by

$$f\,(X) = \phi\,\text{TSP}\,(X) + \text{Dir}\,(X, C)$$

which differs from the original objective function $F(X)$ in (1) in that we have assumed that $\psi = 1$ (without loss of generality) and that $\gamma_k = 0$ for all k. The proof for general sequences $\{\gamma_k\}$ follows the same line of reasoning as this section, and is given in Section E of the online supplement. We re-iterate that we also assume that the input region C is contained in a bounding box of dimensions $(\text{diam}(C) = 1/h = w) \times h$, which implies that $\text{Area}(C) = A \in [1/2, 1]$. Throughout this section we will use the terms w and $1/h$ interchangeably to simplify exposition. To begin, we define the function $\alpha(A)$ as

$$\alpha(A) = H(A, \sqrt{3}, 1/\sqrt{3}) \in (0.2943, 0.4753) \text{ for } A \in [1/2, 1]$$

and the function $\beta(A)$ as

$$\beta(A) = H(A, 1, 1) \in (0.2092, 0.3826) \text{ for } A \in [1/2, 1]$$

which we will abbreviate from now on as α and β, suppressing the dependence on A in the interests of brevity. It is not hard to verify that α and β are concave in A.

Note that Algorithm 3 requires that we iterate through various values of k from 1 through $K = \max\left\{\lfloor 1/h^2 \rceil, \lfloor \alpha/2\phi \rceil\right\}$. In fact, it turns out that we can verify that the desired approximation ratio holds by only checking *three* strategic values of k, namely $k = 1$, $k = \lfloor 1/h^2 \rceil$, and $k = \lfloor \alpha/2\phi \rceil$, which are shown in Figure 17. Since we are assuming that $\psi = 1$ and $\gamma_k = 0$ in this section, we can condense the lower bounding functions Φ^1_{LB} and Φ^2_{LB} to

$$\Phi^1_{\text{LB}}(A, \phi) = \begin{cases} A\sqrt{\phi} - \frac{3\phi\sqrt{\pi A}}{8} & \text{if } \phi \leq \frac{16A}{9\pi} \\ \frac{2A^{3/2}}{3\sqrt{\pi}} & \text{otherwise} \end{cases}$$

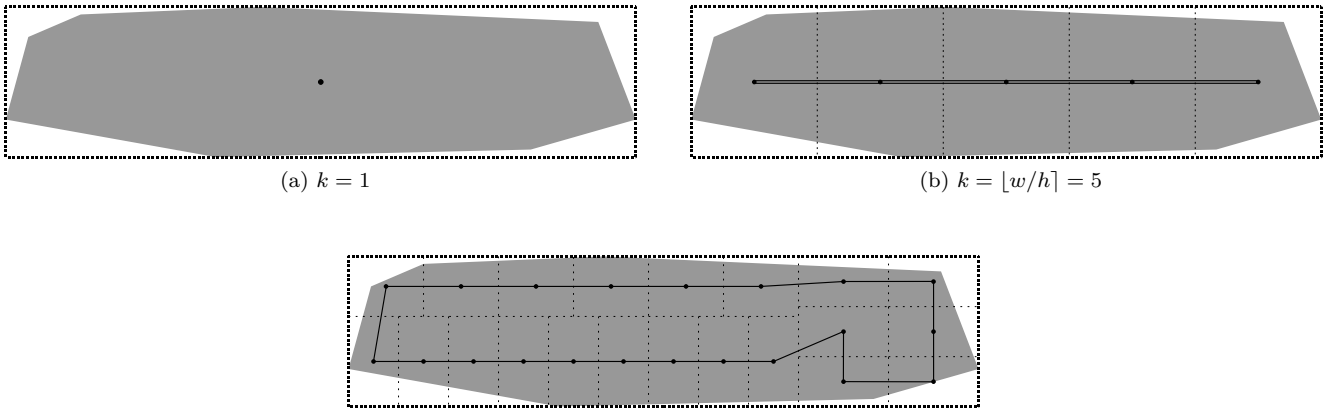

(a) $k = 1$

(b) $k = \lfloor w/h \rfloor = 5$

(c) $k = \lfloor \alpha/2\phi \rfloor = 21$

Figure 17: The three candidate outputs that are passed to Algorithm 2, with TSP paths shown. For visual clarity, the Voronoi diagrams of the point sets have been omitted and instead we show the rectangular partition from Algorithm 1 that led to their placement.

and

$$\Phi^2_{\mathrm{LB}}(A, \phi, h) = \begin{cases} (2A\phi - 4\phi^2)/h & \text{if } \phi \leq \frac{A}{4} \\ \frac{A^2}{4h} & \text{otherwise} \end{cases}$$

where we have used the fact that the assumption that $\gamma_k = 0$ implies that k should be ∞ in our lower bounds (since they are both decreasing in k). We subsequently define $\Phi_{\mathrm{LB}}(A, \phi, h) = \max\{\Phi^1_{\mathrm{LB}}(A, \phi), \Phi^2_{\mathrm{LB}}(A, \phi, h)\}$.

We can define upper bounding functions Φ^1_{UB}, Φ^2_{UB}, and Φ^3_{UB} as follows:

- If we apply Algorithm 2 with only $k = 1$ point, then there is no backbone network and therefore the objective function cost is at most $H(A, 1/h, h)$. We consequently define $\Phi^1_{\mathrm{UB}}(A, \phi, h) = H(A, 1/h, h)$. As mentioned in Claim 18, we have

  $$\Phi^1_{\mathrm{UB}}(A, \phi, h) \sim \frac{2A}{3h} - \frac{1}{12h} - \frac{A^2}{3h}$$

  as $h \to 0$.

- If we apply Algorithm 2 with $k = \lfloor 1/h^2 \rceil = \lfloor w/h \rfloor$ points, then we have a backbone network with length $2 \cdot \frac{k-1}{hk}$ and a collection of k equidistantly spaced points $X = \{x_1, \ldots, x_k\}$, each of which is contained in a rectangle R_i (produced by Algorithm 15) of dimensions $w/k \times h$. By convexity of $H(\cdot)$ in A, we know that the maximum value of $\mathrm{Dir}(X, C)$ is therefore bounded above by $k \cdot H(A/k, w/k, h)$, so that we may define

  $$\Phi^2_{\mathrm{UB}}(A, \phi, h) = 2\left(\frac{k-1}{hk}\right)\phi + k \cdot H\left(\frac{A}{k}, \frac{1}{hk}, h\right)$$

  with $k = \lfloor 1/h^2 \rceil$. Note that as $h \to 0$, the aspect ratios of the rectangles R_i approach 1 (since $\mathrm{AR}(R_i) = \frac{w/k}{h} = \frac{1/h^2}{\lfloor 1/h^2 \rceil} \to 1$), so that

  $$\Phi^2_{\mathrm{UB}}(A, \phi, h) \sim \frac{2\phi}{h} + \frac{\beta}{\sqrt{k}} \sim \frac{2\phi}{h} + \beta h$$

  for small h by applying a simple scaling argument to the definition of β.

- If we apply Algorithm 2 with $k = \lfloor \alpha/2\phi \rceil$ and we also have $\lfloor \alpha/2\phi \rceil \geq 1/3h^2$, then by Claim 20, we know that all of the rectangles $R_1, \ldots, R_k$ produced by Algorithm 15 have an aspect ratio of at most 3. We therefore know that the

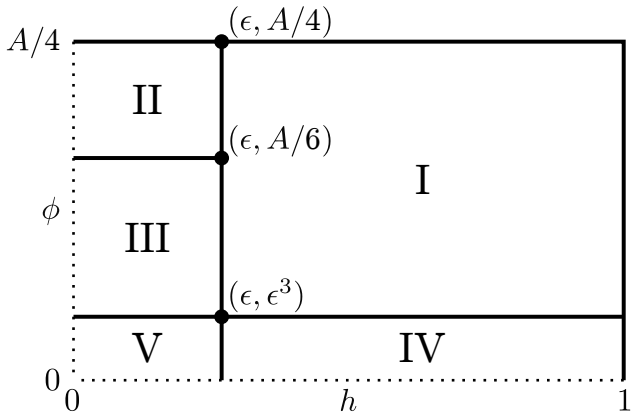

Figure 18: The bounded domain $(\phi, h) \in (0, A/2] \times (0, 1]$, where ϵ is a small quantity (say 10^{-6}), obviously not drawn to scale. Here we assume that $A \in [1/2, 1]$ is fixed and we consider the approximation ratio as a function of ϕ and h; the dashed lines reflect the fact that the domain of interest is open on one end (i.e. we cannot have $h = 0$ or $\phi = 0$).

maximum value of $\mathrm{Dir}(X, C)$ is bounded above by $k \cdot H(A/k, \sqrt{3/k}, 1/\sqrt{3k})$, which is equal to $\alpha/\sqrt{k}$ by applying a simple scaling argument to the definition of α. Using Theorem 15, we can therefore define

$$\Phi^3_{\mathrm{UB}}(A, \phi, h) = \begin{cases} \phi \left\lceil \frac{hk}{m} + \frac{m}{h} + 2\left(\frac{m-1}{m}\right) h \right\rceil + \alpha/\sqrt{k} & \text{if } \lfloor \alpha/2\phi \rceil \geq 1/3h^2 \\ \infty & \text{otherwise}, \end{cases}$$

with $k = \lfloor \alpha/2\phi \rceil$ and $m = 2 \cdot \max\{1, \lfloor \sqrt{\alpha} h/2\sqrt{2\phi} \rceil\}$. Note that as $\phi/h^2 \to 0$, we find that $\Phi^3_{\mathrm{UB}}(A, \phi, h) \sim 2\sqrt{2\alpha\phi}$. The choice of $k = \lfloor \alpha/2\phi \rceil$ rectangles to make our upper bound small follows the same spirit as that of the districting-routing strategy of [12].

We subsequently define

$$\Phi_{\mathrm{UB}}(A, \phi, h) = \min\{\Phi^1_{\mathrm{UB}}(A, \phi, h), \Phi^2_{\mathrm{UB}}(A, \phi, h), \Phi^3_{\mathrm{UB}}(A, \phi, h)\}$$

and we will next show that $\Phi_{\mathrm{UB}}(A, \phi, h)/\Phi_{\mathrm{LB}}(A, \phi, h) \leq 3.93$ for all possible inputs.

6.1 Decomposing the input domain

It is clear that our proof will be complete if we can verify that $\Phi_{\mathrm{UB}}/\Phi_{\mathrm{LB}} \leq 3.93$ on the domain $(A, \phi, h) \in [1/2, 1] \times (0, \infty) \times (0, 1]$. In order to make this domain bounded, we first observe that if $\phi > A/4$ (which is obviously bounded below by $1/8$), then $\Phi^1_{\mathrm{UB}}/\Phi^2_{\mathrm{LB}} \leq 3.4$. This is because neither bound depends on ϕ in this range, so we merely have to check the domain $(A, h) \in [1/2, 1] \times (0, 1]$. We can conclude that $\Phi^1_{\mathrm{UB}}/\Phi^2_{\mathrm{LB}} \leq 3.4$ on this domain by verifying the desired result computationally on the compact domain $(A, h) \in [1/2, 1] \times [\epsilon, 1]$ for small ϵ, then observing that as $h \to 0$ we have

$$\frac{\Phi^1_{\mathrm{UB}}}{\Phi^2_{\mathrm{LB}}} \sim \frac{\frac{2A}{3h} - \frac{1}{12h} - \frac{A^2}{3h}}{\frac{A^2}{4h}} = \frac{8A - 4A^2 - 1}{3A^2} < 3 \text{ for } A \in [1/2, 1]$$

as desired. It will therefore suffice to verify that $\Phi_{\mathrm{UB}}/\Phi_{\mathrm{LB}} \leq 3.93$ on the *bounded* domain $(A, \phi, h) \in [1/2, 1] \times (0, A/4] \times (0, 1]$. We will prove this by decomposing the domain in question into five sub-domains as shown in Figure 18:

- Sub-domain I is compact and has strictly positive values of A, ϕ, and h. Thus, we can verify that $\Phi_{\mathrm{UB}}/\Phi_{\mathrm{LB}} \leq 3.93$ computationally using a branch-and-bound procedure; this is fairly straightforward because all upper and lower bounds are increasing in ϕ and A and decreasing in h. Figure 19 actually shows a surface plot of this ratio so that we can also visually confirm the bound.
- On sub-domain II, we have $\phi \in [A/6, A/4]$ and h small, so that

$$\frac{\Phi^1_{\mathrm{UB}}}{\Phi^2_{\mathrm{LB}}} \sim \frac{\frac{2A}{3} - \frac{1}{12} - \frac{A^2}{3}}{2A\phi - 4\phi^2} \leq \frac{\frac{2A}{3} - \frac{1}{12} - \frac{A^2}{3}}{2A(A/6) - 4(A/6)^2} \leq 3 \text{ for } A \in [1/2, 1].$$

- On sub-domain III, we have ϕ bounded below by ϵ^3 and h small, so that

$$\frac{\Phi^2_{\text{UB}}}{\Phi^2_{\text{LB}}} \sim \frac{2\phi/h + \beta h}{(2A\phi - 4\phi^2)/h} \sim \frac{2\phi/h}{(2A\phi - 4\phi^2)/h} = \frac{1}{A - 2\phi} \leq \frac{1}{A - 2(A/6)} \leq 3 \text{ for } A \in [1/2, 1]\,.$$

- On sub-domain IV, we have $\phi \ll h^2$, so that (provided ϵ is small enough to ensure that $\alpha/2\epsilon^3 > 1/3$, i.e. that Φ^3_{UB} is finite) the approximation ratio is

$$\frac{\Phi^3_{\text{UB}}}{\Phi^1_{\text{LB}}} \sim \frac{2\sqrt{2\alpha\phi}}{A\sqrt{\phi} - \frac{3\phi\sqrt{\pi A}}{8}} \sim \frac{2\sqrt{2\alpha}}{A} < 3.2 \text{ for } A \in [1/2, 1]\,.$$

- On sub-domain V, the analysis is somewhat more involved because ϕ and h are both small but the ratio between them may be arbitrarily large. We consider the family of curves in sub-domain V of the form $\{(\phi, h) : \phi = ch^2\}$ over varying c. If $c \geq 1/8$, then we find that

$$\frac{\Phi^2_{\text{UB}}}{\Phi^2_{\text{LB}}} \sim \frac{2\phi/h + \beta h}{(2A\phi - 4\phi^2)/h} =\sim \frac{1}{A} + \frac{\beta}{2cA} \leq 3.7 \text{ for } A \in [1/2, 1]\,.$$

  If $c < 1/8$, then we find that

$$\frac{\Phi^3_{\text{UB}}}{\Phi^1_{\text{LB}}} = \frac{\phi\left[\frac{hk}{m} + \frac{m}{h} + 2\left(\frac{m-1}{m}\right)h\right] + \alpha/\sqrt{k}}{A\sqrt{\phi} - \frac{3\phi\sqrt{\pi A}}{8}} \sim \frac{4(\alpha/m + 2cm + 4ch^2(1 - 1/m) + 2\sqrt{2\alpha c})}{(8A\sqrt{c} - 3ch\sqrt{A\pi})}$$

  where $m = \lfloor\sqrt{\alpha/2c}\rceil$. As $c \to 0$ and thus $m \to \infty$, the above expression is approximately

$$\frac{4(\alpha/\sqrt{\alpha/2c} + 2c\sqrt{\alpha/2c} + 4ch^2\left[1 - 1/\sqrt{\alpha/2c}\right] + 2\sqrt{2\alpha c})}{(8A\sqrt{c} - 3ch\sqrt{A\pi})} \sim \frac{2\sqrt{2\alpha}}{A} < 3.2 \text{ for } A \in [1/2, 1]\,.$$

  The non-limiting case for c (e.g. $c \in [10^{-3}, 1/8]$) can be handled computationally.

This completes the proof that Algorithm 3 is a factor 3.93 approximation algorithm for minimizing the objective function of (1) for the special case where $\gamma_k = 0$ for all k. In Figure 19 we show a plot of $\Phi_{\text{UB}}/\Phi_{\text{LB}}$ for $A = 1/2$ and $(\phi, h) \in (0, 1/4] \times (0, 1]$.

Theorem 21. *Algorithm 3 is an approximation algorithm for minimizing the objective function of (1), with approximation constant* 3.93*. Its running time is* $\mathcal{O}\left(\omega n + \omega^2 \log n\right)$*, where* $\omega = \max\left\{1/h^2, 1/\phi\right\}$ *and* n *is the number of vertices of* C*.*

Proof. See Section E of the online supplement for a generalization of the preceding proof for general sequences $\{\gamma_k\}$. □

7 Conclusions

We have considered the problem of designing an optimal facility location configuration in a convex planar region to minimize a weighted combination of the fixed costs, backbone network costs, and transportation costs in the region. We first showed that the two asymptotically optimal configurations that minimize these costs are the well-studied honeycomb heuristic and the Archimedes heuristic, which we introduced here. After analyzing several variations on our initial model, we then gave a fast constant-factor approximation algorithm for placing facilities in any convex polygonal region to minimize the costs described herein.

A natural direction for further research would be to investigate the optimal solutions to variations of our problem under different assumptions on the backbone network topology. The results in this paper describe the optimal solutions when the backbone network is a TSP tour or a minimum spanning or Steiner tree, although other possibilities remain, such as a *complete graph* or *star network* on the facilities. We expect the optimal solutions for these problems to have a distinctly different behavior and we intend to study them in the near future.

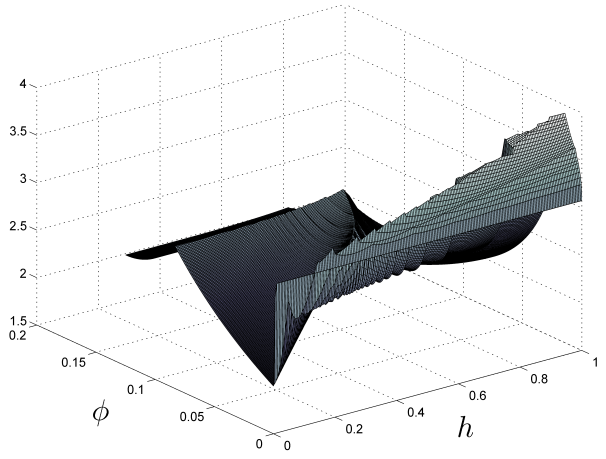

Figure 19: The ratio $\Phi_{\mathrm{UB}}/\Phi_{\mathrm{LB}}$ for $A = 1/2$ and $(\phi, h) \in (0, A/4] \times (0, 1]$.

8 Acknowledgments

The authors wish to thank Gérard Cachon for his initial formulation of this problem and Saif Benjaafar for introducing the topic. The authors also thank Jiawei Zhang, Z. Max Shen, the associate editor, and two anonymous referees for their helpful comments.

Notes

[1] One very minor distinction between our objective function (1) and that of [6] is that the paper [6] does not consider emissions from facilities (the fixed costs $\gamma_{|X|} \cdot |X|$).

[2] The paper [13] actually proves that $\zeta_3 \geq 2/3$, although numerical simulations strongly suggest that equality holds.

References

[1] P. Arnold, D. Peeters, and I. Thomas. Modelling a rail/road intermodal transportation system. *Transportation Research Part E: Logistics and Transportation Review*, 40(3):255 – 270, 2004.

[2] J. Beardwood, J. H. Halton, and J. M. Hammersley. The shortest path through many points. *Mathematical Proceedings of the Cambridge Philosophical Society*, 55(4):299–327, 1959.

[3] P. A. G. Bergeijk and S. Brakman. *The Gravity Model in International Trade: Advances and Applications*. Cambridge University Press, 2010.

[4] O. Berman, P. Jaillet, and D. Simchi-Levi. Location-routing problems with uncertainty. In Z. Drezner, editor, *Facility Location: A Survey of Applications and Methods*, pages 427–452. Springer, 1995.

[5] D. J. Bertsimas and D. Simchi-Levi. A new generation of vehicle routing research: Robust algorithms, addressing uncertainty. *Operations Research*, 44(2), 1996.

[6] G. P. Cachon. Supply chain design and the cost of greenhouse gas emissions. Working paper, 2012.

[7] J. F. Campbell. Designing logistics systems by analyzing transportation, inventory and terminal cost tradeoffs. *Journal of Business Logistics*, 11(1), 1990.

[8] J. F. Campbell. One-to-many distribution with transshipments: An analytic model. *Transportation Science*, 27(4):330–340, 1993.

[9] J. F. Campbell and J. V. Nickerson. Optimal arrangements for assembling a network in an emergency. *Hawaii International Conference on System Sciences*, 0:1–10, 2011.

[10] J.G. Carlsson, F. Jia, and Y. Li. An approximation algorithm for the continuous k-medians problem in a convex polygon. *INFORMS Journal on Computing*, under 3rd round of review. See `http://menet.umn.edu/~jgc/fermat-weber.pdf`.

[11] C. F. Daganzo. The length of tours in zones of different shapes. *Transportation Research Part B: Methodological*, 18(2):135 – 145, 1984.

[12] C. F. Daganzo and G. F. Newell. Configuration of physical distribution networks. *Networks*, 16(2):113–132, 1986.

[13] Z. Drezner and E. Zemel. Competitive location in the plane. *Ann. Oper. Res.*, 40:173–193, February 1993.

[14] L. Few. The shortest path and the shortest road through n points. *Mathematika*, 2:141–144, 1955.

[15] A. M. Geoffrion. Making better use of optimization capability in distribution system planning. *AIIE Transactions*, 11(2):96–108, 1979.

[16] B. Grunbaum and G.C. Shephard. *Tilings and Patterns*. Dover Books on Mathematics Series. Dover Publications, 2012.

[17] M. Haimovich and A. H. G. Rinnooy Kan. Bounds and heuristics for capacitated routing problems. *Mathematics of Operations Research*, 10(4):527–542, 1985.

[18] D. S. Hochbaum. When are NP-hard location problems easy? *Annals of Operations Research*, 1:201–214, 1984.

[19] A. Langevin, P. Mbaraga, and J. F. Campbell. Continuous approximation models in freight distribution: An overview. *Transportation Research Part B: Methodological*, 30(3):163 – 188, 1996.

[20] S. Li. A 1.488 approximation algorithm for the uncapacitated facility location problem. In *Proceedings of the 38th international conference on Automata, languages and programming - Volume Part II*, ICALP'11, pages 77–88, Berlin, Heidelberg, 2011. Springer-Verlag.

[21] T. L. Magnanti and R. T. Wong. Network design and transportation planning: models and algorithms. *Transportation Science*, 18(1):1–55, 1984.

[22] S. Melkote and M. S. Daskin. An integrated model of facility location and transportation network design. *Transportation Research Part A: Policy and Practice*, 35(6):515 – 538, 2001.

[23] P. A. Miranda and R. A. Garrido. Incorporating inventory control decisions into a strategic distribution network design model with stochastic demand. *Transportation Research Part E: Logistics and Transportation Review*, 40(3):183 – 207, 2004.

[24] G. Nagy and S. Salhi. Location-routing: Issues, models and methods. *European Journal of Operational Research*, 177(2):649 – 672, 2007.

[25] G. F. Newell. Scheduling, location, transportation, and continuum mechanics; some simple approximations to optimization problems. *SIAM Journal on Applied Mathematics*, 25(3):pp. 346–360, 1973.

[26] G. F. Newell and C. F. Daganzo. Design of multiple-vehicle delivery tours–I a ring-radial network. *Transportation Research Part B: Methodological*, 20(5):345 – 363, 1986.

[27] M. Pinedo. *Scheduling: theory, algorithms, and systems*. Springer, 2008.

[28] C. Redmond and J. E. Yukich. Limit theorems and rates of convergence for euclidean functionals. *The Annals of Applied Probability*, 4(4):pp. 1057–1073, 1994.

[29] J.P. Rodrigue, C. Comtois, and B. Slack. *The Geography of Transport Systems*. Routledge, 2009.

[30] E. Sheppard. Theoretical underpinnings of the gravity hypothesis. *Geographical Analysis*, 10(4):386–402, 1978.

[31] J. M. Steele. Subadditive euclidean functionals and nonlinear growth in geometric probability. *The Annals of Probability*, 9(3):pp. 365–376, 1981.

[32] E. Zemel. Probabilistic analysis of geometric location problems. *Annals of Operations Research*, 1:215–238, 1984. 10.1007/BF01874390.

Online supplement to "Continuous facility location with backbone network costs"

A Analysis of the Archimedes heuristic

We consider here the limiting behavior of the "Archimedes heuristic" in which facilities are located on an Archimedean spiral with equation given in polar coordinates by $r = a\theta$ for some appropriately chosen a. Suppose that the service region C is a circle with radius $r = 1/\sqrt{\pi}$ (i.e. with area 1). Suppose that we distribute an infinite number of facilities X on an Archimedean spiral with $a = \sqrt{\phi/\psi}/\pi$. Using the arc length formula for Archimedes' spiral, given by

$$s(\theta) = \frac{a}{2}\left[\theta\sqrt{1+\theta^2} + \log\left(\theta + \sqrt{1+\theta^2}\right)\right],$$

it is not hard to show that the travelling salesman tour of these facilities (i.e. the length of the spiral plus the trip back to the center) satisfies

$$\mathrm{TSP}(X) \sim \frac{\sqrt{\psi/\phi}}{2}$$

as $\psi \to \infty$ (the trip back to the center is a constant, roughly equal to $r = 1/\sqrt{\pi}$ and is dwarfed by the other terms). As Figure 4 of this paper suggests, it is clear that the facility-to-customer transportation cost $\mathrm{Dir}(X, C)$ is the same as the Fermat-Weber value of a collection of facilities distributed on a line of length $\sqrt{\psi/\phi}/2$ which is embedded in the middle of a rectangle of dimensions $\sqrt{\psi/\phi}/2 \times 2\sqrt{\phi/\psi}$, which evaluates to

$$\int_{-\sqrt{\phi/\psi}}^{\sqrt{\phi/\psi}} \int_0^{\sqrt{\psi/\phi}/2} |x_2|\, dx_1\, dx_2 = \sqrt{\phi/\psi}/2\,.$$

Thus, we have $\mathrm{TSP}(X) \sim \sqrt{\psi/\phi}/2$ and $\mathrm{Dir}(X, C) \sim \sqrt{\phi/\psi}/2$, whence $\phi\,\mathrm{TSP}(X) + \psi\,\mathrm{Dir}(X) \sim \sqrt{\phi\psi}$ as desired.

B Competitive location when $\gamma_k \in o(k^{-1/2})$

In this section we consider the problem

$$\underset{X}{\text{minimize}}\ \gamma_{|X|} \cdot |X| + (\phi = 1)\,\mathrm{TSP}(X) + \psi \max_{p \in C} S(p\,|X\,)$$

when $\gamma_k \in o(k^{-1/2})$ and the facilities X are placed equidistantly along an Archimedean spiral of length $\ell = 18^{1/3}\psi^{1/3}/3$. From Figure 20, it is clear that as $\psi \to \infty$ (and thus as $\ell \to \infty$), the maximum area that the attacking facility p can steal is

$$\frac{1}{3\ell^2}\left(1 + \mathcal{O}\left(\frac{\ell^4}{k^2}\right)\right) = \frac{1}{3\ell^2} + \mathcal{O}\left(\frac{\ell^2}{k^2}\right)$$

where $k = |X|$ and thus, plugging in our desired value of ℓ, we find that the objective function is then given by

$$\gamma_k \cdot k + (\phi = 1)\ell + \frac{\psi}{3\ell^2} + \mathcal{O}\left(\frac{\psi\ell^2}{k^2}\right) \le \gamma_k \cdot k + c_0\frac{\psi^{5/3}}{k^2} + c\psi^{1/3}$$

where c_0 is some constant and $c\psi^{1/3} \approx 1.310\psi^{1/3}$ is the conjectured optimal cost to problem (4) when facility costs are ignored. Thus, it will suffice to show that if $\gamma_k \in o(k^{-1/2})$, then

$$\min_k \gamma_k \cdot k + c_0\frac{\psi^{5/3}}{k^2} \in o(\psi^{1/3})$$

as $\psi \to \infty$. This proof is basically identical to the proof of Claim 2.

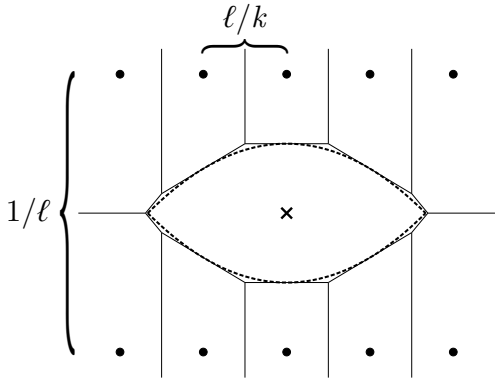

Figure 20: The stolen region $S(p|X)$ when k points are placed equidistantly along the spiral (we assume that ℓ is sufficiently large that the curvature of the spiral does not contribute significantly). The dashed lines indicate the stolen region $S_\infty(p|X)$ when *infinitely* many facilities are placed along the spiral. We can think of $S(p|X)$ as simply being a piecewise linear approximation of $S_\infty(p|X)$, which will have a relative error of $\mathcal{O}((\ell^2/k)^2) = \mathcal{O}(\ell^4/k^2)$.

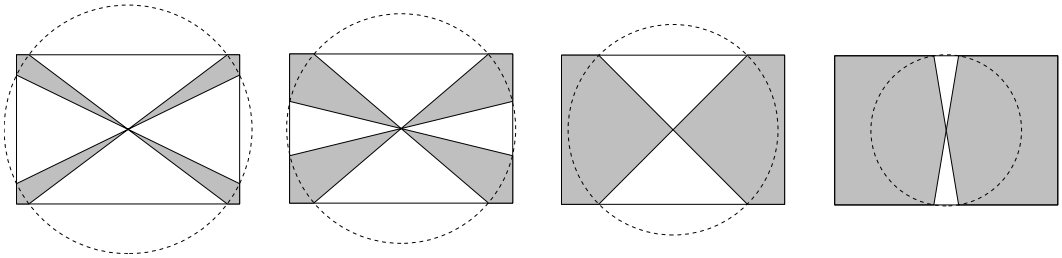

Figure 21: The worst-case regions C^* in a given rectangle R, for increasing values of A.

C Proof of Theorem 17

Definition 22. A region C is said to be *star convex at the point* p if the line segment from p to any point $x \in C$ is itself contained in C. Similarly, the *star convex hull* of a region S at the point p is the smallest star-convex region at the point p that contains S (i.e. the union of all segments between points $x \in S$ and p).

Lemma 23. *Let R be a rectangle of dimensions $w \times h$ centered at the origin. The region C^* that solves the infinite-dimensional optimization problem*

$$\begin{aligned} \underset{C}{\text{maximize}}\, \text{Dir}\,(C) \qquad & s.t. \\ C &\subseteq R \\ \text{Area}\,(C) &= A \\ C &\ni (0,0) \\ C &\text{ is } \text{star convex at } (0,0) \end{aligned} \tag{13}$$

is the star convex hull of $R \backslash D$, where D is an appropriately chosen disk centered at the origin, as indicated in Figure 21. Furthermore for fixed w and h, the function $\Phi(A) = \text{Dir}\,(C^*)$ (i.e. the maximal value of (13)) is monotonically increasing and concave.

Proof sketch. This follows from a standard argument where we consider the integer (or linear) program obtained by discretizing problem (13) using polar coordinates. See Figure 22a. Concavity of $\Phi(A)$ follows by observing that we build our optimal solution by adding sectors containing points that are strictly closer than the points in the sector that preceded them. □

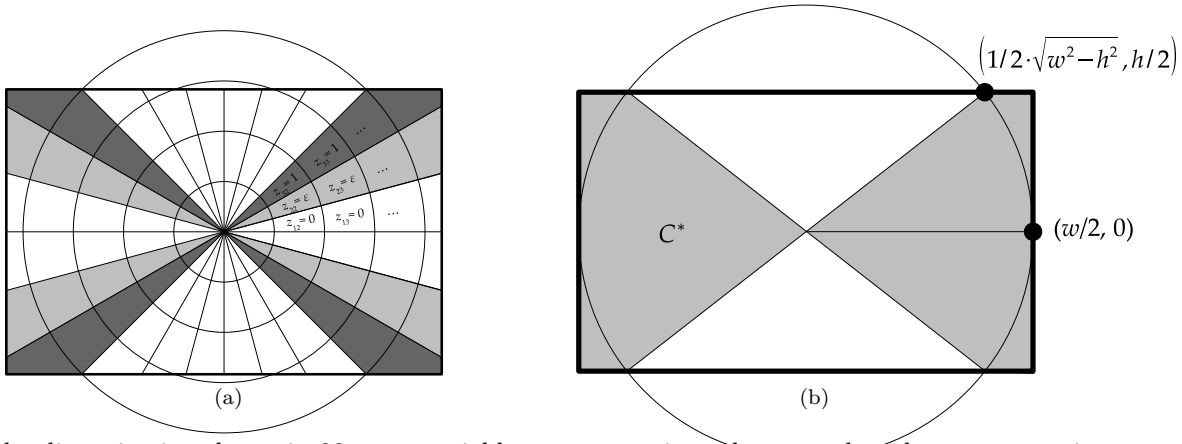

Figure 22: In the discretization shown in 22a, our variables are set up in such a way that the star convexity constraint is equivalent to setting $z_{i(j+1)} \leq z_{ij}$ for all j. Since we are finding an upper bound of the Fermat-Weber value of a star-convex object in the given box, our objective is to maximize $\sum_{i,j} d_{ij} z_{ij}$ subject to the constraints that $\sum_{i,j} a_{ij} z_{ij} = A$, $z_{i(j+1)} \leq z_{ij}\, \forall i, j$, and $z_{ij} \geq 0\, \forall i, j$, where d_{ij} denotes the distance from the origin to cell ij and a_{ij} denotes the area of cell ij. By the nature of the constraints it is clear that we may assume that $z^*_{i(j+1)} = z^*_{ij}$ at optimality since the distance from cell ij to the origin increases with j. The diagram above suggests a linear programming formulation, where the lighter regions indicate fractional solutions. Figure 22b shows the necessary value of A for which the region C^* consists of only two regions instead of four; the area of the shaded region is $wh - \frac{h}{2}\sqrt{w^2 - h^2}$.

In order to prove Theorem 17 we consider the infinite-dimensional optimization problem of choosing the worst-case convex region C that solves the problem

$$\begin{aligned} \underset{C}{\text{maximize}}\, \text{Dir}\,(C) \qquad & s.t. \\ C &\subseteq R \\ \text{Area}\,(C) &= A \\ C &\ni (0,0) \\ C &\text{ is convex.} \end{aligned}$$

By relaxing the convexity constraint with star convexity about the origin, the problem becomes equivalent to problem (13); we can use it to determine an upper bound on $\text{Dir}(C)$.

Following Lemma 23 we see that the worst-case star-convex region C^* takes the form shown in Figure 21. If $A \geq wh - \frac{h}{2}\sqrt{w^2 - h^2}$, then the optimal solution consists of two components (rather than 4) as shown in Figure 22b. The bound given in Theorem 17 is precisely the Fermat-Weber value $\iint_{C^*} ||x||\, dA$ obtained by analytic integration. We can prove Remark 18 by taking the Fermat-Weber values of C^* under the ℓ_1 and ℓ_∞ norms instead (which have a much simpler closed form) and observing that

$$\iint_{C^*} ||x||_1\, dA \sim \frac{2}{3}Aw - \frac{1}{12}w^2 h - \frac{1}{3}\cdot\frac{A^2}{h}$$

and

$$\iint_{C^*} ||x||_\infty\, dA \sim \frac{2}{3}Aw - \frac{1}{12}w^2 h - \frac{1}{3}\cdot\frac{A^2}{h}$$

from which (12) holds by the squeeze theorem.

D Proof of Claim 20

To prove Claim 20 it is sufficient to show that the following lemma holds:

Lemma 24. *Suppose that $\tilde{R} \subseteq \square C$ is an intermediate rectangle obtained throughout Algorithm 1, which is further subdivided into $\tilde{R}'$ and $\tilde{R}''$. Then:*

1. If $\mathrm{AR}(\tilde{R}) > 3$, then
$$\mathrm{AR}(\tilde{R}'), \mathrm{AR}(\tilde{R}'') \leq \mathrm{AR}(\tilde{R})\,.$$
2. If $\mathrm{AR}(\tilde{R}) \leq 3$, then
$$\mathrm{AR}(\tilde{R}'), \mathrm{AR}(\tilde{R}'') \leq 3\,.$$

Proof. Claim 1 is trivial. To prove Claim 2 we assume that $\mathrm{AR}(\tilde{R}) \leq 3$. Assume without loss of generality that $\mathrm{width}(\tilde{R}) \geq \mathrm{height}(\tilde{R})$, so that $\mathrm{height}(\tilde{R}') = \mathrm{height}(\tilde{R})$. Since $\tilde{R}$ is always divided into proportions as close as $1/2$ as possible, we have
$$\mathrm{width}(\tilde{R})/3 \leq \mathrm{width}(\tilde{R}') \leq 2\,\mathrm{width}(\tilde{R})/3$$
and, dividing by $\mathrm{height}(\tilde{R})$, we find that
$$\frac{\mathrm{width}(\tilde{R})}{3\,\mathrm{height}(\tilde{R})} \leq \frac{\mathrm{width}(\tilde{R}')}{\mathrm{height}(\tilde{R}')} = \frac{\mathrm{width}(\tilde{R}')}{\mathrm{height}(\tilde{R})} \leq \frac{2\,\mathrm{width}(\tilde{R})}{3\,\mathrm{height}(\tilde{R})} \leq 2$$
so that $\mathrm{width}(\tilde{R}')/\,\mathrm{height}(\tilde{R}') \leq 2$. Taking the reciprocal of this expression and observing that $3 \geq 3\,\mathrm{height}(\tilde{R})/\,\mathrm{width}(\tilde{R})$ since $\mathrm{width}(\tilde{R}) \geq \mathrm{height}(\tilde{R})$, we have
$$3 \geq \frac{3\,\mathrm{height}(\tilde{R})}{\mathrm{width}(\tilde{R})} \geq \frac{\mathrm{height}(\tilde{R}')}{\mathrm{width}(\tilde{R}')} = \frac{\mathrm{height}(\tilde{R})}{\mathrm{width}(\tilde{R}')} \geq \frac{3\,\mathrm{height}(\tilde{R})}{2\,\mathrm{width}(\tilde{R})}$$
so that $3 \geq \mathrm{height}(\tilde{R}')/\,\mathrm{width}(\tilde{R}')$. This same argument clearly applies to $\tilde{R}''$ as well, which completes Claim 2. □

E Proof of Theorem 21

In this section we give a sketch of the complete proof of Theorem 21 by showing that Algorithm 3 is a factor 3.93 approximation algorithm for minimizing objective function (1) when $\{\gamma_k\}$ is nonzero. Recall that Algorithm 3 merely iterates Algorithm 2 through potential values of $|X|$ from 1 to $K := \max\{\lfloor \alpha/2\phi \rceil, \lfloor 1/h^2 \rceil\}$ and then selects the X with the best found objective value $F(X)$. Let X^* denote the *true* optimal solution that minimizes (1), and note that (depending on $\{\gamma_k\}$) we may have $|X^*| = \infty$. If $|X^*| > K$, then we claim that Algorithm 3 is guaranteed to have the same factor 3.93 approximation as in the case where $\gamma_k = 0$ everywhere. This is because, if we let $\bar{X}$ denote the best-found solution from Algorithm 3, then we have
$$\begin{aligned}
\frac{F(\bar{X})}{F(X^*)} = \frac{\gamma_{|\bar{X}|}\cdot|\bar{X}| + \phi\,\mathrm{TSP}\left(\bar{X}\right) + \mathrm{Dir}\left(\bar{X}, C\right)}{\gamma_{|X^*|}\cdot|X^*| + \phi\,\mathrm{TSP}\left(X^*\right) + \mathrm{Dir}\left(X^*, C\right)} &\leq \frac{\gamma_{|X^*|}\cdot|X^*| + \phi\,\mathrm{TSP}\left(\bar{X}\right) + \mathrm{Dir}\left(\bar{X}, C\right)}{\gamma_{|X^*|}\cdot|X^*| + \phi\,\mathrm{TSP}\left(X^*\right) + \mathrm{Dir}\left(X^*, C\right)} \\
&\leq \frac{\phi\,\mathrm{TSP}\left(\bar{X}\right) + \mathrm{Dir}\left(\bar{X}, C\right)}{\phi\,\mathrm{TSP}\left(X^*\right) + \mathrm{Dir}\left(X^*, C\right)} \\
&= \frac{f(\bar{X})}{f(X^*)} \leq 3.93
\end{aligned}$$
where we have used the fact that $\gamma_{|X^*|}\cdot|X^*| \geq \gamma_{|\bar{X}|}\cdot|\bar{X}|$ because $\gamma_k \cdot k$ is an increasing sequence. Thus, it will suffice to consider the case where $|X^*| \leq K$. More specifically, letting $k^* = |X^*|$, we will consider the problem
$$\underset{X}{\text{minimize}}\, f(X) := \phi\,\mathrm{TSP}(X) + \mathrm{Dir}(X, C) \qquad s.t.\, |X| \leq k^*$$

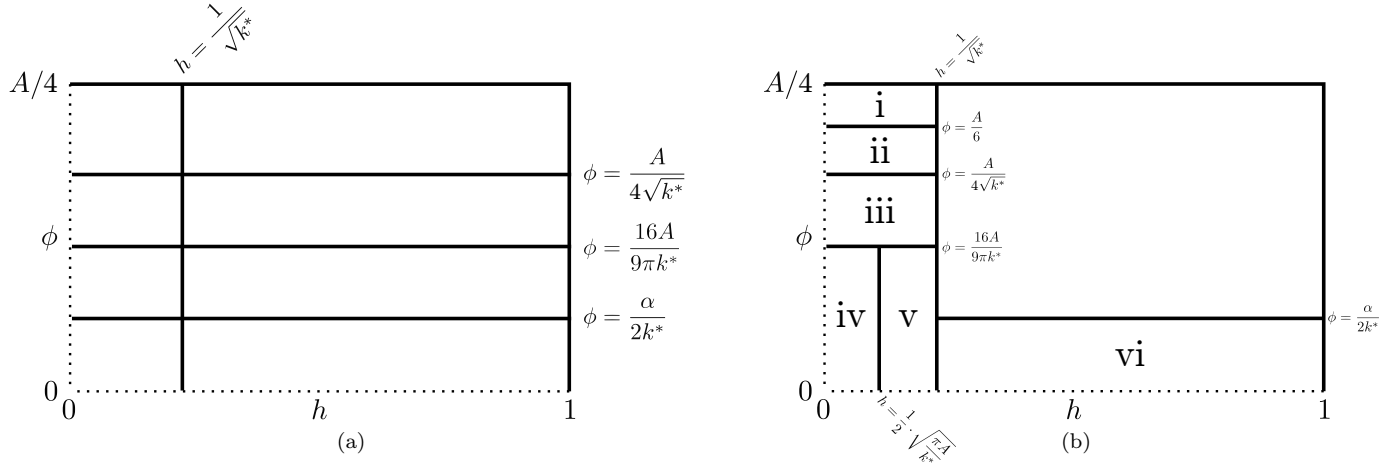

Figure 23: Subdomains (not drawn to scale) on which our upper bounding function is affected because $\phi < \alpha/2k^*$ or $h < 1/\sqrt{k^*}$.

and show that Algorithm 3 will always produce a solution $\bar{X}$ whose objective value $f(\bar{X})$ is within a factor of 3.93 of the objective value $f(X^*)$. This will prove our claim because

$$\frac{\gamma_{|\bar{X}|} \cdot |\bar{X}| + f(\bar{X})}{\gamma_{k^*} \cdot k^* + f(X^*)} \leq \frac{\gamma_{k^*} \cdot k^* + f(\bar{X})}{\gamma_{k^*} \cdot k^* + f(X^*)} \leq \frac{f(\bar{X})}{f(X^*)} \leq 3.93\,.$$

As in Section 6, we will consider at most three candidate values of k, namely $k = 1$, $k = \min\{k^*, \lfloor 1/h^2 \rceil\}$, and $k = \min\{k^*, \lfloor \alpha/2\phi \rceil\}$.

E.1 Proving bounds

In this section we will show that, if we apply Algorithm 2 with $k = 1$, $k = \min\{k^*, \lfloor 1/h^2 \rceil\}$, and $k = \min\{k^*, \lfloor \alpha/2\phi \rceil\}$, then we are guaranteed to find a solution $\bar{X}$ whose objective value $f(\bar{X})$ is within a factor of 3.93 of the optimal objective value $f(X^*)$ as in the previous section. We begin by altering the lower bounds (8) and (9) slightly, incorporating our assumption that $\psi = 1$ and omitting the contributions of the form $\gamma_k \cdot k$ (which we are safe in doing, since we are considering the ratio $f(\bar{X})/f(X^*)$ which does not depend on these contributions)

$$\Phi^1_{\mathrm{LB}}(A, \phi, k) = \begin{cases} \frac{3\sqrt{A\pi}}{8}(\sqrt{k} - 1)\phi + \frac{2A^{3/2}\psi^{3/2}}{3\sqrt{\pi k}} & \text{if } \phi \leq \frac{16A}{9\pi k} \\ A\sqrt{\phi} - \frac{3\phi\sqrt{\pi A}}{8} & \text{if } \frac{16A}{9\pi k} < \phi \leq \frac{16A}{9\pi} \\ \frac{2A^{3/2}}{3\sqrt{\pi}} & \text{otherwise} \end{cases}$$

$$\Phi^2_{\mathrm{LB}}(A, \phi, h, k) = \begin{cases} \frac{2(1+1/\sqrt{k})A}{h}\phi + \frac{A^2}{4hk} & \text{if } \phi \leq \frac{A}{4\sqrt{k}} \\ \frac{2\phi A}{h} - \frac{4\phi^2}{h} & \text{if } \frac{A}{4\sqrt{k}} < \phi \leq \frac{A}{4} \\ \frac{A^2}{4h} & \text{otherwise} \end{cases}$$

It is obvious that the lower bounds above are decreasing in k. It is also clear that our upper bounds are only affected (i.e. they differ from the upper bounds in Section 6) when either $k^* < \lfloor \alpha/2\phi \rceil$ or $k^* < \lfloor 1/h^2 \rceil$. Since k^* is an integer, we may drop the rounding terms in the conditions $k^* < \lfloor \alpha/2\phi \rceil$ and $k^* < \lfloor 1/h^2 \rceil$ to obtain the equivalent constraints that $\phi < \alpha/2k^*$ and $h < 1/\sqrt{k^*}$ as shown in Figure 23a. We may therefore restrict our attention only to the subdomains marked (i) through (vi) in Figure 23b, since the upper bounding function is unaffected outside those subdomains (and the lower bounding function can only *increase* as a result of incorporating bounds in k). We can address these using precisely the same technique as in Section 6 and we omit the case-by-case study for brevity.